THE JOURNAL OF BIOLOGICAL CHEMISTRY VOL. 286, NO. 10, pp. 8308–8324, March 11, 2011

Zymophagy, a Novel Selective Autophagy Pathway Mediated by VMP1-USP9x-p62, Prevents Pancreatic Cell Death*◆

Received for publication, October 26, 2010, and in revised form, December 9, 2010 Published, JBC Papers in Press, December 20, 2010, DOI 10.1074/jbc.M110.197301

Daniel Grasso[‡1], Alejandro Ropolo[‡], Andrea Lo Ré[‡2], Verónica Boggio[‡], María I. Molejón[‡3], Juan L. Iovanna[§], Claudio D. Gonzalez[‡], Raúl Urrutia[¶], and María I. Vaccaro[‡4]

From the [‡]Department of Pathophysiology, School of Pharmacy and Biochemistry, University of Buenos Aires, C1113AAD Buenos Aires, Argentina, the [§]Unité 624, INSERM, 13288 Marseille, France, and the [¶]Chromatin Dynamics and Epigenetic Laboratory, Mayo Clinic, Rochester, Minnesota 55905

Autophagy has recently elicited significant attention as a mechanism that either protects or promotes cell death, although different autophagy pathways, and the cellular context in which they occur, remain to be elucidated. We report a thorough cellular and biochemical characterization of a novel selective autophagy that works as a protective cell response. This new selective autophagy is activated in pancreatic acinar cells during pancreatitis-induced vesicular transport alteration to sequester and degrade potentially deleterious activated zymogen granules. We have coined the term "zymophagy" to refer to this process. The autophagy-related protein VMP1, the ubiquitin-protease USP9x, and the ubiquitin-binding protein p62 mediate zymophagy. Moreover, VMP1 interacts with USP9x, indicating that there is a close cooperation between the autophagy pathway and the ubiquitin recognition machinery required for selective autophagosome formation. Zymophagy is activated by experimental pancreatitis in genetically engineered mice and cultured pancreatic acinar cells and by acute pancreatitis in humans. Furthermore, zymophagy has pathophysiological relevance by controlling pancreatitis-induced intracellular zymogen activation and helping to prevent cell death. Together, these data reveal a novel selective form of autophagy mediated by the VMP1-USP9x-p62 pathway, as a cellular protective response.

Autophagy is an evolutionarily preserved cellular process that is responsible for the degradation of long lived proteins and entire organelles to maintain intracellular homeostasis and to contribute to starvation and stress responses. Macroautophagy involves the formation of double-membrane autophagosomes around cargoes, including larger structures such as organelles and protein aggregates. Autophagosomes then fuse with lysosomes, where the degradation of the cargoes takes place. Both nonselective "bulk" autophagy and selective autophagy of specific proteins and organelles have been described (1). Genetic analyses in yeast identified more than 30 conserved components that are required for different steps of autophagy (termed Atg1 to Atg32) (2). Several lines of evidence suggest the existence of different types of selective autophagic degradation pathways. Single proteins and cellular structures such as protein aggregates, peroxisomes, ribosomes, and mitochondria can be specifically engulfed by autophagosomes (3), but the mechanism of cargo recognition is not well understood. However, there is emerging evidence suggesting the involvement of ubiquitin in this process. For example, aggregate clearance by autophagy requires ubiquitylation and ubiquitin-binding receptors such as p62 (also known as SQSTM1) (4). Ubiquitylated artificial substrates are recognized by the autophagy machinery and are specifically degraded in lysosomes by a p62-dependent mechanism (5). Moreover, the selective degradation of excess ribosomes during starvation depends on the deubiquitylation activity of Ubp3/Bre5 (6). However, the repertoire of proteins that participate in these ubiquitin-mediated pathways during different types of autophagy remains an area of intensive investigation, particularly to elucidate the role of this specific cellular program in pathophysiological processes, such as defects in vesicular traffic in pancreatitis.

We have previously reported the identification of the vacuole membrane protein-1 (VMP1) in pancreatitis affected acinar cells and positioned it as a new autophagy-related protein. VMP1 induces autophagosome formation, even under nutrient-replete conditions while remaining an integrated autophagosomal membrane protein in mammalian cells (7). VMP1 interacts with Beclin 1/ATG6 through its hydrophilic C-terminal region (VMP1-Atg domain), which is necessary for early steps of autophagosome formation (7). The latter has also been reported by Tian *et al.* (8) by identifying EPG-3/VMP1 as one of three essential autophagy genes conserved from worms to mammals, which regulates early steps of the autophagic pathway in *Caenorhabditis elegans*. Hierarchical analyses in mammalian cells by Itakura and Mizushima (9) showed that VMP1 along with ULK1 and Atg14 localize in the endoplasmic reticulum-associated autophagosome formation sites in a PI3K activity-independent manner, confirming the key role of VMP1 in the formation of autophagosomes. Interestingly, *Dictyostelium* cells lacking *Vmp1* gene showed accumulation of huge ubiquitin-positive protein aggregates

* This work was supported in part by the Agencia Nacional de Promoción Científica y Tecnológica Grant ANPCyT-PICT01627, Consejo Nacional de Investigaciones Científicas y Técnicas Grant CONICET-PIP2527, and the University of Buenos Aires Grant UBA-UBACyTM072.
◆ This article was selected as a Paper of the Week.
[1] University of Buenos Aires Fellow.
[2] Consejo Nacional de Investigaciones Cientificas y Técnicas fellow.
[3] Agencia Nacional de Promoción Cientifica y Tecnológica Fellow.
[4] To whom correspondence should be addressed: School of Pharmacy and Biochemistry, University of Buenos Aires, 956 Junín, C1113AAD Buenos Aires, Argentina. Tel.: 5411-4964-8368; Fax: 5411-4968-8268; E-mail: mvaccaro@ffyb.uba.ar.

containing the autophagy marker Atg8/LC3 and p62 homolog (10). Despite the progress made in VMP1-mediated autophagy, whether this process cooperates with the ubiquitin pathway remains to be firmly established.

The pancreatic acinar cell is a highly polarized, differentiated cell whose primary function is the synthesis and secretion of digestive enzymes into the pancreatic juice. Pancreatic digestive enzymes are produced as inactive enzymes (zymogens) and stored in subcellular structures called zymogen granules, until exocytosis. Zymogen granules are potentially harmful because activated digestive enzymes are able to hydrolyze tissue parenchyma. Acute pancreatitis, defined as the pancreas self-digestion, is the most frequent disease of the pancreas. During pancreatitis, ultrastructural alterations of zymogen granules are produced in a yet undefined way. These alterations are characterized by premature activation of trypsinogen to trypsin within pancreatic acinar cells leading to the progression of the disease (11). We have previously demonstrated that VMP1 autophagic vesicles are present in the pancreas of rats submitted to experimental pancreatitis (7), suggesting that VMP1 is involved in the induction of autophagy during the disease. Considering that autophagy is implicated in several pathological mechanisms operating in human diseases, it remains unknown whether the VMP1 pathway regulates potential pathophysiological processes.

Cholecystokinin is a pancreatic secretagogue that interacts with G_q-coupled receptors in the acinar cell to induce pancreatic secretion in physiological conditions. However, the hyperstimulation of cholecystokinin receptors (CCK-R)[5] with the analog cerulein modifies vesicular transport and leads to intracellular proteolytic enzyme activation and ultimately cell death (12). These cellular events are characteristic of acute pancreatitis. Therefore, in this study, we use this secretagogue-induced model because it is the most commonly employed and best characterized model of acute pancreatitis (12).

The results from our work describe the critical function of autophagy in secretory granule homeostasis and cell response to injury by the selective degradation of altered secretory granules in acute pancreatitis. This process, which we define as "zymophagy," can be induced by the hyperstimulation of CCK-R in a transgenic mouse model for studying VMP1-induced autophagy in pancreatic acinar cells (ElaI-VMP1 mice). Zymophagy degrades the activated granules avoiding the release of their contents into the cytoplasm, thus preventing further trypsinogen activation and cell death. We report that the ubiquitin-binding protein p62, which is a cargo receptor for selective autophagy, participates in VMP1-mediated autophagy. We also describe in ElaI-VMP1 mice the immunomagnetic isolation of autophagosomes containing zymogen granules induced by CCK-R hyperstimulation. Furthermore, we demonstrate that zymophagy requires a physical interaction between the ubiquitin-protease USP9x and VMP1, supporting a previously unidentified key role for the ubiquitin pathway. We also show the induction of VMP1 expression and zymophagy in human pancreas affected by acute pancreatitis. These results demonstrate a previously unrecognized function for VMP1, mediating zymophagy, a novel selective form of autophagy, which functionally links the autophagy pathway with the ubiquitin machinery to trigger a protective response to cell death.

[5] The abbreviations used are: CCK-R, cholecystokinin receptor; BZiPAR, rhodamine 110 bis-(CBZ-L-isoleucyl-L-prolyl-L-arginine amide) dihydrochloride; 3-MA, 3-methyladenine; EGFP, enhanced GFP.

EXPERIMENTAL PROCEDURES

Transgenic Mice (ELAI-VMP1 Mice)—The transgene cassette was made using the pBEG vector (7, 13). The expression cassette contains the acinar-specific control region (−500 to +8) from the rat elastase I gene and the human growth hormone 3′-untranslated region (UTR) (+500 to +2657). This construct was digested with BamHI, filled in, dephosphorylated, and ligated with rat VMP1-EGFP released from pEGFP-VMP1 plasmid. A 1940-kb HindIII/NotI fragment was isolated and used for microinjections into inbred FVB zygotes. Genomic DNA was prepared and tested by Southern blot and PCR.

Cerulein-induced Pancreatitis—Male C57BL6J and C57BL6J-ElaI-VMP1 mice weighing 20–25 g were used. Animals were housed with free access to food and water. Experiments were performed according to the standard ethical and legal guidelines of the University of Buenos Aires regulations for animal experiments. Pancreatitis was induced by seven intraperitoneal injections of cerulein (Sigma) (50 μg/kg) given at 1-h intervals; mice were killed by decapitation at different times after the first injection. In one series of experiments, the pancreata were removed, homogenized in HEPES buffer, pH 7.4, containing protease inhibitors (0.5 mM PMSF, 5 μg/ml pepstatin, 5 μg/ml leupeptin, and 2.5 μg/ml aprotinin), and processed for Western blot analysis. In another series of experiments, the pancreata were removed and fixed in 4% *p*-formaldehyde for histological analysis or in 2.5% glutaraldehyde for electron microscopy.

Transmission Electron Microscopy—Samples were fixed and processed for transmission electron microscopy by standard procedures. Grids were examined under a Carl Zeiss C-10 electron microscope (LANAIS-MIE, UBA).

Antibodies—Polyclonal rabbit antiserum to VMP1 against the peptide MAQSYAKRIQQRLNSEEKTK (residues 385–406) was obtained and used at 1:100 dilution. Polyclonal goat anti-LC3, goat anti-p62, goat anti-USP9x, goat anti-Lamp2, rabbit anti-trypsinogen, goat anti-amylase, monoclonal mouse anti-GFP antibody (Santa Cruz Biotechnology), and monoclonal mouse anti-V5 (Invitrogen) antibodies were used according to the manufacturer. Alexa Fluor 488 and 594 antibodies (Molecular Probes) were used for immunofluorescence assays. Peroxidase-labeled anti-rabbit and anti-goat IgG antibodies were used for Western blot according to GE Healthcare.

VMP1-EGFP-coated Vesicle Immunoisolation—Enriched organelle fractions were isolated from ElaI-VMP1 mouse pancreata according to the separate methods of Cox and Emili (14) with some modifications. Mouse pancreata were removed and immediately homogenized in 1 ml of ice-cold 250-STM buffer (250 mM sucrose, 50 mM Tris, pH 7.4, 5 mM $MgCl_2$, plus 1 mM PMSF, 10 g/ml leupeptin, 0.5 mg/ml soy-

bean trypsin inhibitor, 20 nM aprotinin, 1 μg/ml pepstatin, and 1 mM benzamidine). The homogenate was centrifuged at 800 × *g* for 10 min to obtain a postnuclear supernatant. Immunoisolations were done as reviewed by Howell *et al.* (15). Briefly, tosylated superparamagnetic beads (Dynabeads M-500 Subcellular; Dynal Inc.) were incubated overnight at room temperature on a rotator with a rabbit anti-mouse linker antibody (ZyMax, Zymed Laboratories Inc., Invitrogen) at a concentration of 10 μg of Ab/mg beads in borate buffer (10 mM H3B3, pH 9.5). For this and all subsequent steps, beads were collected with a magnetic device (MPC, Dynal Inc.). Beads were rinsed with incubation buffer (PBS containing 2 mM EDTA, 5% FBS) for 30 min, Tris buffer (50 mM Tris, pH 7.8, 100 mM NaCl, 0.1% Tween 20, 0.05% BSA) for 60 min, and incubation buffer for 30 min. Coated Dynabeads (2–10 mg) were incubated for 12 h on a rotator with mouse anti-GFP monoclonal antibody (Santa Cruz Biotechnology) at a concentration of 10 μg/mg beads diluted in incubation buffer to a final volume of 1 ml. To obtain beads for control experiments, coated beads were incubated as above in incubation buffer alone. Beads (2–10 mg) were rinsed with two changes of incubation buffer and then incubated overnight at 4 °C on a rotator with 0.15–0.25 mg of postnuclear supernatant (25–30 μg of protein/mg of beads) in 1 ml of incubation buffer. Beads were then collected, rinsed with incubation buffer, and saved as the inmunoisolated fractions and alternatively processed by standard transmission electron microscopy technique or by Western blot assay. To quantify immunoisolated autophagosomes, 100 magnetic beads were evaluated, and all beads attached to vesicles were counted. The vesicles were classified as empty vesicles (empty or unspecific cargo containing vesicles) or zymogen granules containing vesicles. Results were expressed as percentage of total number of vesicles counted and represented as mean ± S.D. of three independent experiments.

Pancreatic Acini Isolation—Pancreatic acini were prepared by collagenase digestion of pancreata and suspended in HEPES-Ringer buffer with Eagle's minimal essential amino acids, 1 mg/ml BSA, and equilibrated with 100% O_2. Viability of acini was 95% based on trypan blue exclusion (16). *In vitro* cerulein-induced amylase secretion was made as acini functional evaluation. Acini from both ElaI-VMP1 and wild type mice were incubated at 37 °C with varying concentrations of cerulein for 30 min. Amylase secretion into the medium and total amylase content of the samples were measured. Net stimulated amylase secretion was calculated as the difference between the percentage of total amylase secreted in the presence and absence of cerulein (17). An *in vitro* CCK-R hyperstimulation model of acute pancreatitis was performed by incubating dispersed pancreatic acini at 37 °C in HEPES-Ringer buffer with 100 nM cerulein (18). Alternatively, acini were incubated with 0.1 nM chloroquine or 0.05 nM vinblastine (Sigma) before being subjected to CCK-R hyperstimulation.

Immunofluorescence Assays—After cerulein treatment, isolated acini and differentiated AR42J cells were fixed during 15 min with 4% *p*-formaldehyde in PBS and immediately washed several times with PBS. Acini were incubated with primary antibodies overnight at 4 °C, according to the manufacturer. Samples were mounted in 1,4-diazabicyclo[2.2.2]octane (Sigma) with DAPI (Sigma) as the nuclear marker and observed in an inverted LSM Olympus FV1000 using an UPLSAPO 60X O NA: 1.35 objective.

Histological Studies—Quantification of inflammatory infiltration was performed on pancreatic tissue sections stained with hematoxylin and eosin (H&E) and expressed as inflammatory cells per 100 acinar cells. Alternatively, tissues were fixed in 1% glutaraldehyde in 0.1 M phosphate buffer and stained with 1% toluidine blue in borax for necrosis quantification. Cells with swollen cytoplasm, loss of plasma membrane integrity, and leakage of organelles into interstitium were considered necrotic; and results expressed as necrotic cells per 100 acinar cells.

Trypsin Activity Assays—Fluorescent microscopy for observation of trypsin activity, isolated acini, and differentiated AR42J cells were incubated 20 min in extracellular solution containing 100 μM rhodamine 110 bis-(CBZ-L-isoleucyl-L-prolyl-L-arginine amide) dihydrochloride (BZiPAR) (Invitrogen) in HEPES buffer, pH 7.5, and observed immediately. To quantify the trypsin activity, isolated pancreatic acini and differentiated AR42J cells were lysed, and 20 μg of protein of each sample were mixed with 100 μl of 4 mM trypsin substrate butoxycarbonyl-Gln-Ala-Arg-7-amido-4-methylcoumarin hydrochloride (Sigma), in trypsin reaction buffer (10 mM Tris, 20 mM $CaCl_2$, pH 7.4), and then incubated 30 min at 37 °C. The fluorescence intensity from trypsin substrate was measured at 450 nm in a fluorescence microplate reader under excitation at 380 nm.

Myeloperoxidase Quantification—Myeloperoxidase activity was measured to quantify neutrophil sequestration. Enzymatic extracts were prepared from pancreas homogenates as described by Dawra *et al.* (19). Myeloperoxidase activity was determined by spectrophotometric method with 3,3′,5,5′-tetramethylbenzidine at 655 nm of absorbance (20).

Differentiated AR42J Acinar Cells, Transfections and Treatments—Rat pancreatic acinar AR42J cells (pancreatoma, ATCC CRL 1492) were cultured in Dulbecco's modified Eagle's medium (Hyclone) supplemented with 10% fetal bovine serum (Invitrogen) and antibiotics (100 units/ml penicillin and 100 μg/ml streptomycin). For differentiation induction, cells were treated with dexamethasone (Sigma) at a final concentration of 100 nM for 48 h (21). Cells were transfected using FuGENE 6 reagent (Roche Applied Science) with the following plasmids: pcDNA4-V5-His (Invitrogen); pEGFP-N1 (Clontech) containing full-length rat VMP1 cDNA (NM_138839); pRFP-C1 containing full-length rat LC3 kindly provided by Dr. María I. Colombo (UNCu-CONICET, Argentina); GFP-Ub (Addgene plasmid 11928) (22) and mRFP-Ub (Addgene plasmid 11935) (23) from Dr. Nico Dantuma (Karolinska Institutet, Sweden). VMP1 and USP9x down-regulation was made by the plasmid pCMS3-H1p-EGFP, which was kindly provided by Dr. D. Billadeau (Department of Immunology, College of Medicine, Mayo Clinic). The plasmid contains a short hairpin RNA construction (for VMP1, sense 5′-GGCAGAAUAUUGUCCUGUGtt-3′ and antisense 5′-CACAGGACAAUAUUCUCUGCCtt-3′; for USP9x, sense 5′-TCCGA-

TGAGGAACCTGCATtt-3′ and antisense 5′-ATGCAGGTTCCTCATCTTT-3′) or a scramble sequence and a separate transcriptional cassette for EGFP to identify transfected cells (24). Differentiated cells were treated with 7.5 μM cerulein (Sigma) to induce CCK-R hyperstimulation. For autophagy inhibition, cells were treated with 10 mM 3-methyladenine (3-MA) (Sigma) 2 h before and during experiments. The efficacy of 3-MA treatment was verified on starved cells (data not shown). Starvation-induced autophagy was stimulated by amino acid/serum-deprived medium using Earle's balanced salts (Invitrogen). For lysosomal hydrolase inhibition, cells were treated with 0.1 nM chloroquine (Sigma) for 1 h before assays.

Percentage of Cells with Punctate LC3 Staining—The percentage of cells with punctate LC3 staining was determined in three independent experiments and expressed as the mean ± S.D. of combined results. To quantify cells with LC3 punctate staining, six random fields representing 100 cells were counted. We consider a cell with punctate LC3 staining when all the LC3 fluorescence is present as punctate and no diffused protein remain. For human pancreas specimens, an arbitrary classification among heterogeneous tissue areas was made before quantification. A_0 was assigned to tissue areas where acini were present in normal morphology. A_1 was assigned to affected areas in which edema, cell detachment, and loss of cell polarity were observed. The quantification of autophagy in human specimens was performed as a percentage of cells with both VMP1-positive staining and punctate LC3, per 100 acinar cells in A_0 and A_1 areas. Staining was counted in six random fields and expressed as mean ± S.D. of three independent experiments.

Coimmunoprecipitation Assays—Dexamethasone-differentiated AR42J cells were transfected with pcDNA4-VMP1-V5-His_6 expression plasmid. Cells were lysed (Lysis buffer: 50 mM Na_2HPO_4, 300 mM NaCl, pH 8.0, 0.5% Tween 20, 0.5% Triton X-100, 10 mM imidazole), and cell lysates were incubated with 50 μl of nickel-nitrilotriacetic acid beads (Qiagen) for 3 h at room temperature; afterward, the supernatant was removed and saved as unbound fraction (S1). nickel-nitrilotriacetic acid beads were intensively washed with lysis buffer and 20 mM imidazole (the second wash was saved as W2). The bound proteins were eluted by lysis buffer supplemented with 200 mM imidazole (E1). Samples were resolved on SDS-PAGE and detected by the appropriate antibodies. For coimmunoprecipitation of endogenous proteins, cell were lysed in lysis buffer containing 137 mM NaCl, 2 mM EDTA, 10% glycerol, 1% Nonidet P-40, 20 mM Tris, pH 8.0, and 5% (v/v) protease inhibitor mixture (Sigma). After preclearance by centrifugation at 14,000 rpm for 10 min, the extracts were incubated with anti-VMP1 antibody at 4 °C overnight. The immunocomplexes were captured by protein G-Sepharose beads (Amersham Biosciences), which were washed five times with lysis buffer. The bound proteins were eluted by 5× SDS sample buffer at 100 °C for 5 min, resolved on SDS-PAGE, and detected by the anti-USP9x antibody (Santa Cruz Biotechnology).

Human Pancreas Specimens—Samples were kindly provided by Dr. Ana Cabane from the Pathology Department, Dr. Carlos Bonorino Udaondo Gastroenterology Hospital, and the study was approved by the Institutional Review Board.

Statistics—Experimental groups were compared using *t* test for pairwise comparisons. For all experiments, statistical significance is indicated as follows: NS, nonsignificant; *, $p < 0.05$; **, $p < 0.001$.

RESULTS

Hyperstimulation of CCK-R in Acinar Cells Induces the Formation of Autophagosomes Containing Zymogen Granules and the Redistribution of VMP1—We initially employed cellular and biochemical tools to characterize the cargo of VMP1-mediated autophagosomes in the context of CCK-R hyperstimulation with cerulein, as a model of pancreatitis. We developed the ElaI-VMP1 mouse in which acinar cell-specific constitutive expression of a VMP1-EGFP chimera induces the formation of autophagosomes (7). We used this unique tool to investigate the role of the VMP1 pathway in autophagy. The ultrastructural features of pancreatic acinar cells from ElaI-VMP1 and wild type mouse specimens, before and after CCK-R hyperstimulation, were studied by electron microscopy (EM). In the untreated mice, both wild type and ElaI-VMP1, acinar cells showed secretory granules with normal ultrastructural characteristics (Fig. 1*A*). CCK-R hyperstimulation in wild type animals induced a markedly altered distribution pattern of the secretory granules. Fig. 1*B* shows intracellular fusion among zymogen granules as well as their fusion with condensing vacuoles. In addition, acinar cells lose their polarity, which results in the relocation of zymogen granules to the basolateral membrane (Fig. 1*B*). All these alterations in vesicular traffic are known to occur in acinar cells during acute pancreatitis and upon hyperstimulation of their CCK-R with cerulein. A comparative EM analysis of ElaI-VMP1 mice subjected to CCK-R hyperstimulation revealed that acinar cells preserve their structure and polarity with negligible or no alteration in vesicular transport. Surprisingly, in pancreata from cerulein-treated ElaI-VMP1 mice, we observed autophagosomes containing zymogen granules displaying a distinct localization to the apical area of the acinar cell. These autophagosomes, containing secretory granules, were easily identifiable in apical regions as round high density structures within double membrane vesicles (Fig. 1, *C–E*). After a systematic observation, we did not find evidence of other subcellular structures, such as ribosomes or mitochondria, within these autophagosomes. These studies also showed different maturation levels of selective autophagic vesicles, providing evidence that autophagic flow remains primarily unchanged under CCK-R hyperstimulation. Examples of large autophagosomes containing morphologically altered zymogen granules and autolysosomes with partially degraded zymogen granules are shown in Fig. 1*F*. Therefore, in acinar cells from the ElaI-VMP1 mice, CCK-R hyperstimulation induces a progressive flow of autophagic vesicles containing zymogen granules that accumulate at the apical pole of acinar cells. Subsequently, we determined the integrity of the mammalian protein p62 (25, 26), which is selectively degraded by autophagy (4). Western blot analysis showed that p62 displays a markedly increased degradation rate in treated ElaI-VMP1

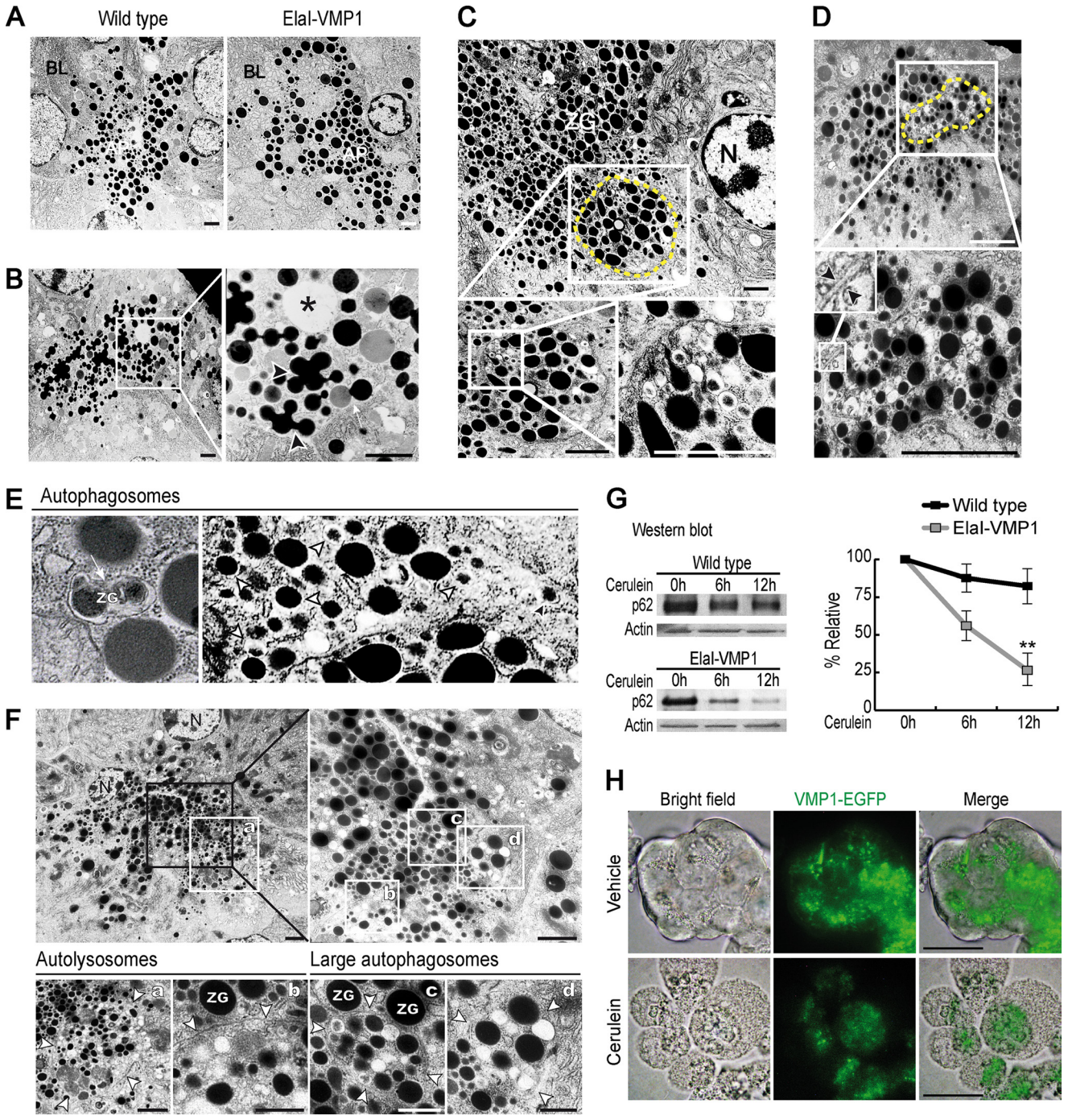

FIGURE 1. **Hyperstimulation of CCK-R in acinar cells induces the redistribution of zymogen granules and VMP1-containing autophagosomes.** *A–F,* transmission electron microscopy of pancreatic tissue. *A,* wild type and Elal-VMP1 mouse pancreata. No ultrastructural alteration is evident in zymogen granules of acinar cells from Elal-VMP1 compared with wild type mouse pancreata. *B,* wild type mouse pancreas after CCK-R hyperstimulation (detailed on the *right*). Ultrastructural alterations of zymogen granules (*arrowheads*), fusion between zymogen granules and condensing vacuoles (*arrow*), and zymogen granules appearing near basolateral dilated space are shown (*). *C–F,* ultrastructure of pancreatic tissue from Elal-VMP1 mice after CCK-R hyperstimulation with cerulein. *C* and *D,* autophagosomes containing zymogen granules are observed in the apical area of the acinar cell (*dashed line*). Zymogen granules inside autophagosomes are detailed in *C* (*bottom panel*). Autophagosome-double membrane is detailed in *D, bottom panel* (*arrowhead*). *E, left panel,* example of zymogen granules sequestered by autophagosome (*arrow*). *Right panel,* examples of autophagosomes containing one single zymogen granule (*arrowheads*). *F,* examples of large autophagosomes and autolysosomes containing zymogen granules. Higher magnification is shown on the *right upper panel*. At the *bottom panel,* the *arrowheads* show the limits of the single membrane autolysosomes (*panels a* and *b*) and large double membrane-limited autophagosomes (*panels c* and *d*). *G,* Western blot analysis and densitometry quantification of p62 in Elal-VMP1 mouse pancreas homogenates shows the progressive reduction of the p62 signal evidencing autophagic flow in pancreas from transgenic mice under CCK-R hyperstimulation with cerulein (**, $p < 0.001$ *versus* wild type). *H,* bright field, VMP1-EGFP fluorescence and merge images of isolated Elal-VMP1 pancreatic acini. VMP1-EGFP fluorescence is located in the basal region of untreated acini (*upper panel*). After 1 h of CCK-R hyperstimulation with cerulein, VMP1-EGFP relocated to the granular area of acinar cells (*bottom panel*). Results are representative of at least three independent experiments. *Scale bars*, 4 μm (*A–F*), and 10 μm (*H*). *BL,* basolateral, *AP,* apical, *ZG,* zymogen granules. *N,* nucleus.

mouse pancreata compared with treated wild type mice (Fig. 1*G*). Thus, these results support the EM analysis described above, suggesting that secretory granules are sequestered and degraded by an autophagic pathway in acinar cells. In addition, it confirms the appropriate functionality of the autophagic flow induced by CCK-R hyperstimulation in the ElaI-VMP1 mouse pancreas.

To gain an insight into a potential codistribution of VMP1 with organelles, which may be the subject of autophagy, we isolated pancreatic acini from ElaI-VMP1 mice. In these specimens, VMP1 can be visualized by direct fluorescence of the VMP1-EGFP chimera expressed in acinar cells. Interestingly, similar to the case of *in vivo* autophagosomes, *in vitro* CCK-R hyperstimulation of ElaI-VMP1 mouse isolated acini also induced a subcellular change in VMP1 localization. Fig. 1*H* shows that VMP1 was distributed at the basal region in untreated acinar cells, but after CCK-R hyperstimulation, VMP1 relocated to the zymogen granule-rich area (apical pole). These results further suggest that under CCK-R hyperstimulation, VMP1-containing autophagosomes relocate to the apical pole to sequester zymogen granules.

Identification of an Inducible and Selective Degradation Process of Zymogen Granules That Involves VMP1 and p62-containing Autophagosomes—We investigated the functional significance of the relocation of VMP1-containing autophagosomes. We first performed immunofluorescence assays using anti-LC3 to identify autophagosomes and anti-trypsinogen to indicate zymogen granules. Fig. 2*A* shows that CCK-R hyperstimulation induced colocalization of LC3 and trypsinogen, indicating that the VMP1-containing autophagosomes relocate to sequester zymogen granules. To further confirm that a VMP1-mediated autophagic process selectively sequesters zymogen granules under CCK-R hyperstimulation, we performed subcellular fractionation studies. We immunopurified VMP1-mediated autophagosomes from ElaI-VMP1 mouse pancreata using anti-GFP antibody bound to magnetic beads. Fig. 2*B* shows that autophagosomes containing zymogen granules were magnetically isolated from the pancreas of ElaI-VMP1 mice treated with cerulein, whereas in untreated animals, either empty or cytoplasm-containing autophagosomes were purified (Fig. 2*C*). Through quantitative analysis, we found that in untreated animals less than 20% of the autophagosomes contain zymogen granules, whereas in the cerulein-treated ones, this percentage increases up to 70% (Fig. 2*D*). Moreover, combined with Western blot analysis, this method allowed us to further identify the cargo of VMP1 autophagosomes. LC3-II, an autophagy-related protein that specifically attaches to autophagosomal membranes, was present in the autophagosomal fraction obtained from both cerulein-treated and untreated specimens, further confirming that an autophagic pathway is involved in the sequestration of zymogen granules (Fig. 2*E*). Notably, strong signals of p62 and trypsinogen were found only in magnetically immunopurified autophagosomes from cerulein-treated ElaI-VMP1 mice (Fig. 2*E*). This finding suggests that p62, which is a ubiquitin-binding protein that interacts with LC3 (4), may function as a cargo receptor during the selective autophagic pathway. Together, the results show that a nonselective autophagy pathway, which involves LC3-II but not p62, is triggered by VMP1 expression in untreated mouse pancreata. On the other hand, upon CCK-R hyperstimulation, p62 is involved in VMP1-mediated selective autophagy of zymogen granules. Thus, as we mentioned earlier, we named this new process of selective autophagy as zymophagy to differentiate it from other types of autophagy.

Zymophagy Selectively Sequesters Activated Zymogen Granules to Prevent the Spreading of Activated Trypsin within the Acinar Cell—To examine the functional relevance of zymophagy, we examined the intracellular activation of trypsinogen in isolated murine pancreatic acini. Isolated acini have been a classical tool for studying organelle movement when vesicular transport is altered by hyperstimulation of CCK-R as a model of acute pancreatitis (15). During transport alteration, there is a sustained increase of intracellular Ca^{2+} concentrations leading to cytoplasmic autoactivation of trypsin in the acinar cell (27). We measured trypsin activity as a surrogate marker for zymogen granule activation, using rhodamine 110 bis-(CBZ-L-isoleucyl-L-prolyl-L-arginine amide) dihydrochloride (BZiPAR), a cell-permeable substrate that becomes fluorescent after the cleavage by this protease (28–30). Trypsin activity was detected by fluorescence of the hydrolyzed substrate within isolated acini. Upon CCK-R hyperstimulation, acinar cells from wild type mice showed early cytoplasmic trypsinogen activation (Fig. 3*A*). In contrast, acinar cells from ElaI-VMP1 mice showed almost no activation of trypsinogen (Fig. 3*B*). These results suggest that the constitutive activation of VMP1-mediated autophagy, characteristic of acinar cells from ElaI-VMP1 mice, prevents intracellular trypsinogen activation in acute pancreatitis. Fig. 3*C* shows the time course of trypsinogen activation, expressed as a relative percentage of maximal trypsin activity after CCK-R hyperstimulation. Under these conditions, wild type acini displayed 45% of maximal trypsin activity after 0.5 h of CCK-R hyperstimulation and reached the 100% activation peak after 1 h. Conversely, acini from ElaI-VMP1 mice only reached 34% of maximal trypsin activity after 1 h treatment. Furthermore, microscopy examinations revealed only few punctate structures containing hydrolyzed substrate restricted to the granular area of acinar cells from ElaI-VMP1 mice. These activated granules colocalized with the VMP1-EGFP fluorescent signal (Fig. 3*D*). Therefore, our results demonstrate that zymophagy is induced during pancreatic acinar cell injury to selectively sequester the activated zymogen granules.

Zymogen activation is an enzymatic chain reaction where initial zymogen granule alterations trigger the rapid spread of active trypsin within the acinar cell. We hypothesized that the degradation of early activated zymogen granules by zymophagy prevents this deleterious event. To test this hypothesis, we evaluated trypsin activity in isolated acini treated with either vinblastine or chloroquine compounds that inhibit autophagic flow by two different mechanisms as follows: interruption of autophagosome-lysosome fusion and inactivation of lysosomal hydrolases, respectively. Thus, we quantified trypsin activation after 1 h of CCK-R hyperstimulation in ElaI-VMP1 mouse acini treated with these inhibitors (Fig. 3, *E* and *F*). Interestingly, these experiments demonstrated that

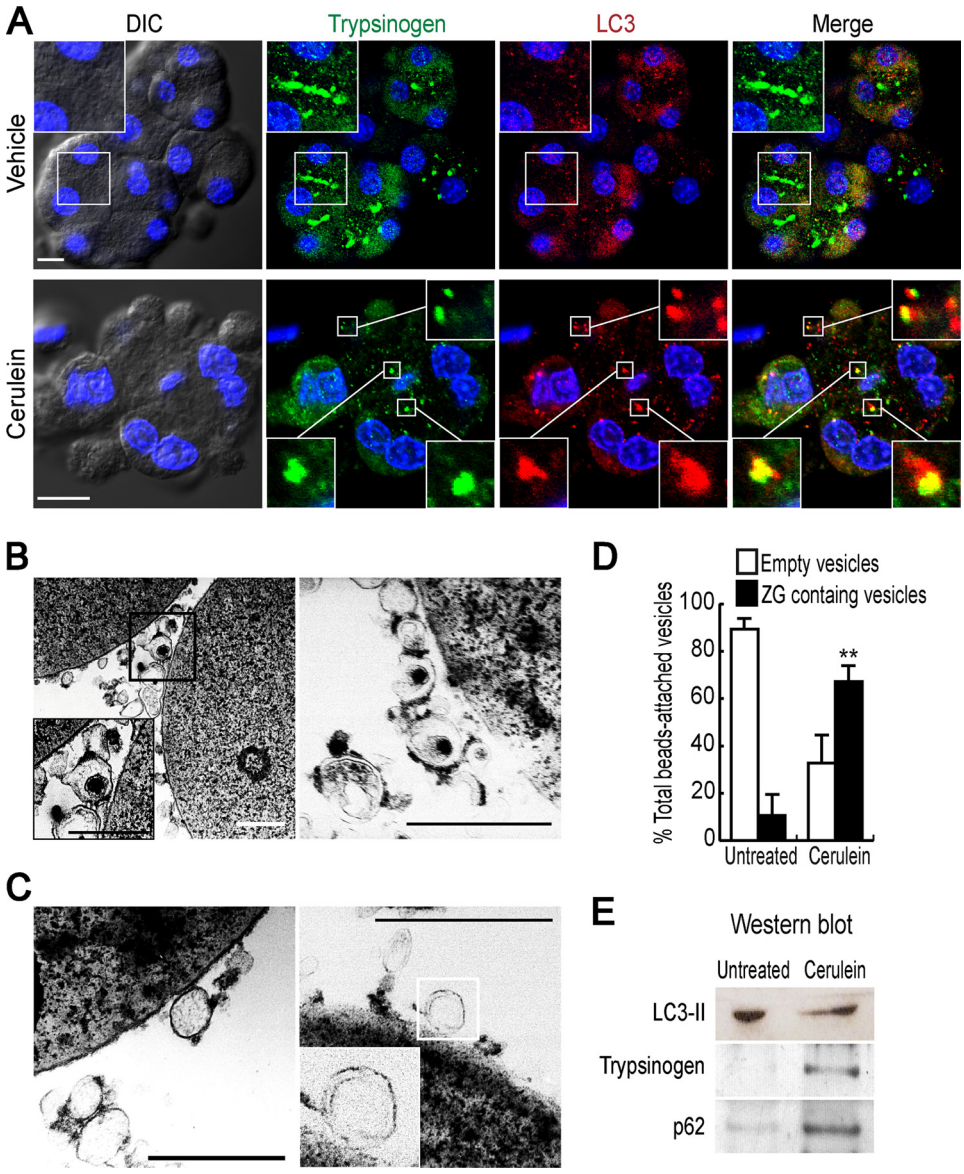

FIGURE 2. **Inducible and selective sequestration of zymogen granules by VMP1-mediated autophagic pathway.** *A,* immunofluorescence assay using anti-LC3 and anti-trypsinogen antibodies on pancreatic acini isolated from ElaI-VMP1 mice. *Top row,* untreated isolated acini. No colocalization between LC3 and trypsinogen is observed in acinar cells. A detail of granular areas is shown on the *upper left side*. *Bottom row,* cerulein-mediated CCK-R hyperstimulated isolated acini. Remarkable colocalization between LC3 and zymogen granules is found in acinar cells. Colocalization examples are detailed. *DIC*, differential interference contrast. *B–D,* isolation of autophagosomes using anti-GFP antibody bound magnetic beads from postnuclear supernatant of ElaI-VMP1 mouse pancreas homogenates. *B*, we show two examples of VMP1-EGFP autophagosomes containing zymogen granules isolated from CCK-R hyperstimulated mouse pancreas homogenates. These double membrane structures containing zymogen granules are detailed in *left panel*. *C*, two examples of VMP1-EGFP-coated structures from untreated ElaI-VMP1 mouse pancreas homogenates. Empty or cytoplasm-containing simple or double membrane structures are observed and detailed (*right panel*). *D*, quantitative analysis indicates that less than 20% of autophagosomes containing zymogen granules are isolated from untreated animal pancreata, and more than 70% of autophagosomes containing zymogen granules are isolated from CCK-R hyperstimulated mouse pancreata (**, $p < 0.001$ *versus* untreated). *E,* Western blot analysis using anti-LC3, anti-trypsinogen, and anti-p62 antibodies of magnetically immunopurified autophagosomes from CCK-R-hyperstimulated ElaI-VMP1 mouse pancreas homogenates (*cerulein lane*) compared with autophagosomal fraction obtained from untreated mouse pancreas (*untreated lane*). The presence of LC3-II (16 kDa) confirms that all the isolated structures are autophagosomes. Zymogen granules as cargo of such autophagosomes are evidenced by trypsinogen-positive blot in autophagosomal fraction isolated from CCK-R-hyperstimulated mouse pancreas. The presence of p62 suggests selective autophagosomes and p62-mediated cargo recognition. Results are representative of at least three independent experiments. *Scale bars,* 10 μm (*A*), and 0.5 μm (*B* and *C*).

the inhibition of autophagic flow markedly increased trypsin activity within acinar cells in ElaI-VMP1 mouse pancreata. These results confirm that zymophagy specifically degrades those zymogen granules that are initially activated by acute pancreatitis preventing the irreversible spreading of activated trypsin into the acinar cell cytoplasm, a phenomenon that ultimately leads to cell death.

Zymophagy Protects Acinar Cells from Intracellular Trypsinogen Activation Triggered in Vivo by Experimental Pancreatitis—Activated trypsin within the acinar cell is considered to contribute importantly to the deleterious effects of acute pancreatitis (31). Consequently, we evaluated the pathophysiological relevance of zymophagy during cerulein-induced acute pancreatitis in mice (32). We first monitored aci-

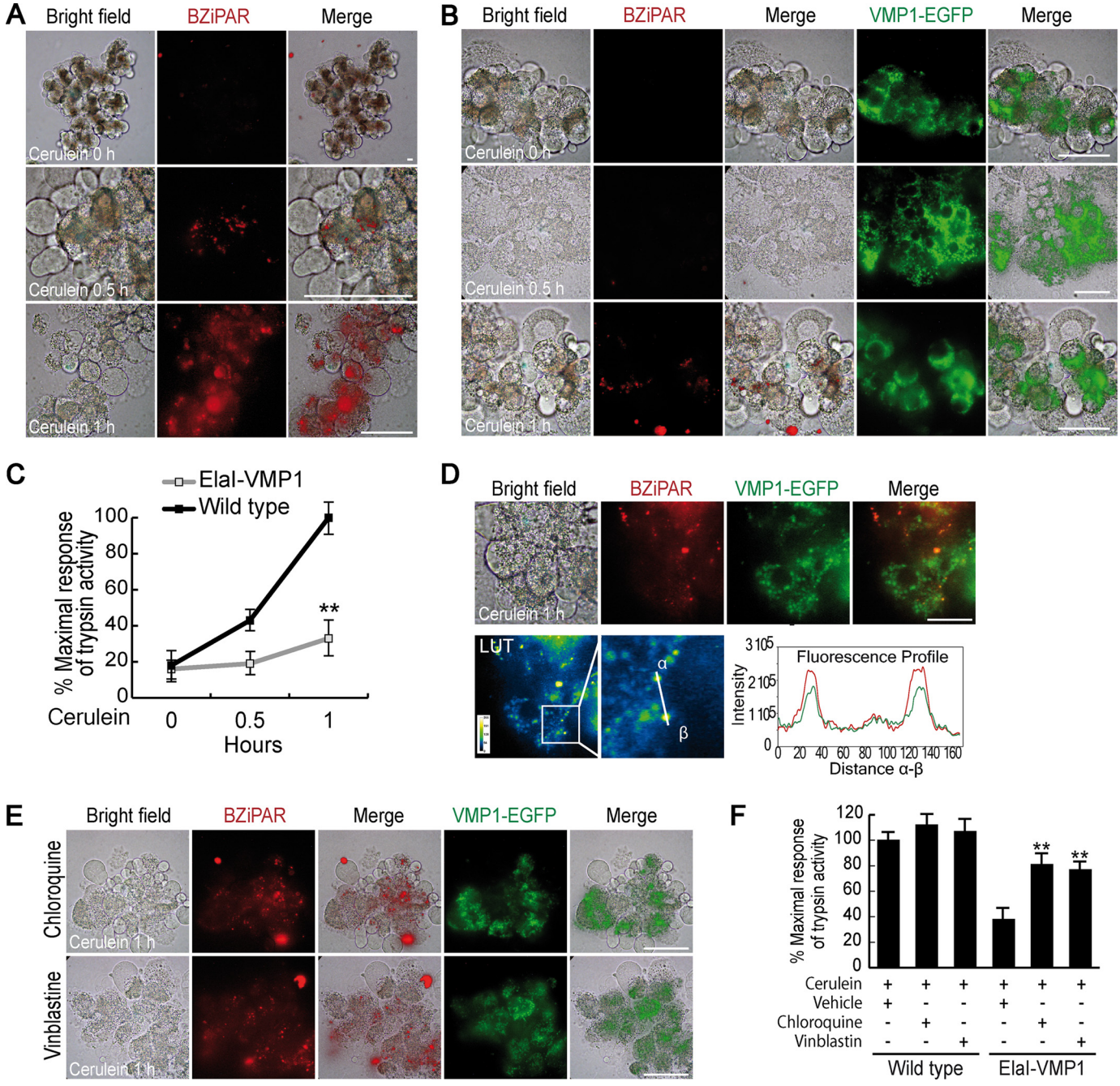

FIGURE 3. **Zymophagy is induced by CCK-R hyperstimulation to selectively sequester and degrade activated zymogen granules.** Intracellular activation of trypsinogen in isolated pancreatic acini was detected by BZiPAR reagent (see "Experimental Procedures"). *A* and *B,* trypsin activity in isolated pancreatic acini before (*top row*), 30 min after (*middle row*), and 1 h after (*bottom row*) cerulein CCK-R hyperstimulation. Activated trypsin is evidenced by *red spots* of hydrolyzed substrate. *A,* acini from wild type mice; early trypsinogen activation is evident within acinar cells during the course of CCK-R hyperstimulation. *B,* acini from ElaI-VMP1 mice; no activity of trypsin is found after 30 min of CCK-R hyperstimulation, and only few spots of hydrolyzed substrate are detected within acinar cells after 1 h of treatment. EGFP-VMP1 fluorescence shows relocation of VMP1 to the granular area of acinar cells in ElaI-VMP1 pancreatic acini after CCK-R hyperstimulation. *C,* quantification of trypsin activity in homogenates from isolated pancreatic acini during CCK-R hyperstimulation. Acini from ElaI-VMP1 mice show significantly less trypsinogen activation compared with wild type mice (**, $p < 0.001$ *versus* wild type). *D,* remarkable colocalization between hydrolyzed trypsin substrate (*red spots*) and VMP1-EGFP fluorescent signals is seen in acinar cells from ElaI-VMP1 mice after 1 h of CCK-R hyperstimulation. Merge image in look-up table (*LUT*) pseudocolor and two hot fluorescence spots profile are shown to prove specific colocalization. *E,* trypsinogen activation in ElaI-VMP1 pancreatic acini treated with chloroquine or vinblastine after 1 h of CCK-R hyperstimulation. *Red* fluorescence spots show increased trypsin activity within acinar cells submitted to both autophagy inhibitory treatments (chloroquine and vinblastine). *F,* trypsinogen activation was quantified as percentage of maximal trypsin activity in wild type mice pancreatic acini under cerulein CCK-R hyperstimulation. The protective effect of VMP1-autophagy pathway on trypsinogen activation in ElaI-VMP1 acini upon cerulein CCK-R hyperstimulation (ElaI-VMP1 vehicle bar) is significantly reversed by autophagy inhibitors (chloroquine and vinblastine treatment bars); (**, $p < 0.001$ *versus* ElaI-VMP1 vehicle bar). No significant differences are observed between vehicle and autophagic flow inhibitors in wild type acini treated with cerulein. *Error bars* indicate standard deviation of at least three independent experiments. *Scale bars,* 20 μm.

nar cell injury using enzymatic markers, such as serum amylase and lipase activities (Fig. 4*A*). No significant differences of these serum enzymatic patterns were found in untreated mice (wild type and ElaI-VMP1 mice). Upon CCK-R hyperstimulation, wild type mice developed acute pancreatitis with high amylase and lipase serum levels. On the contrary,

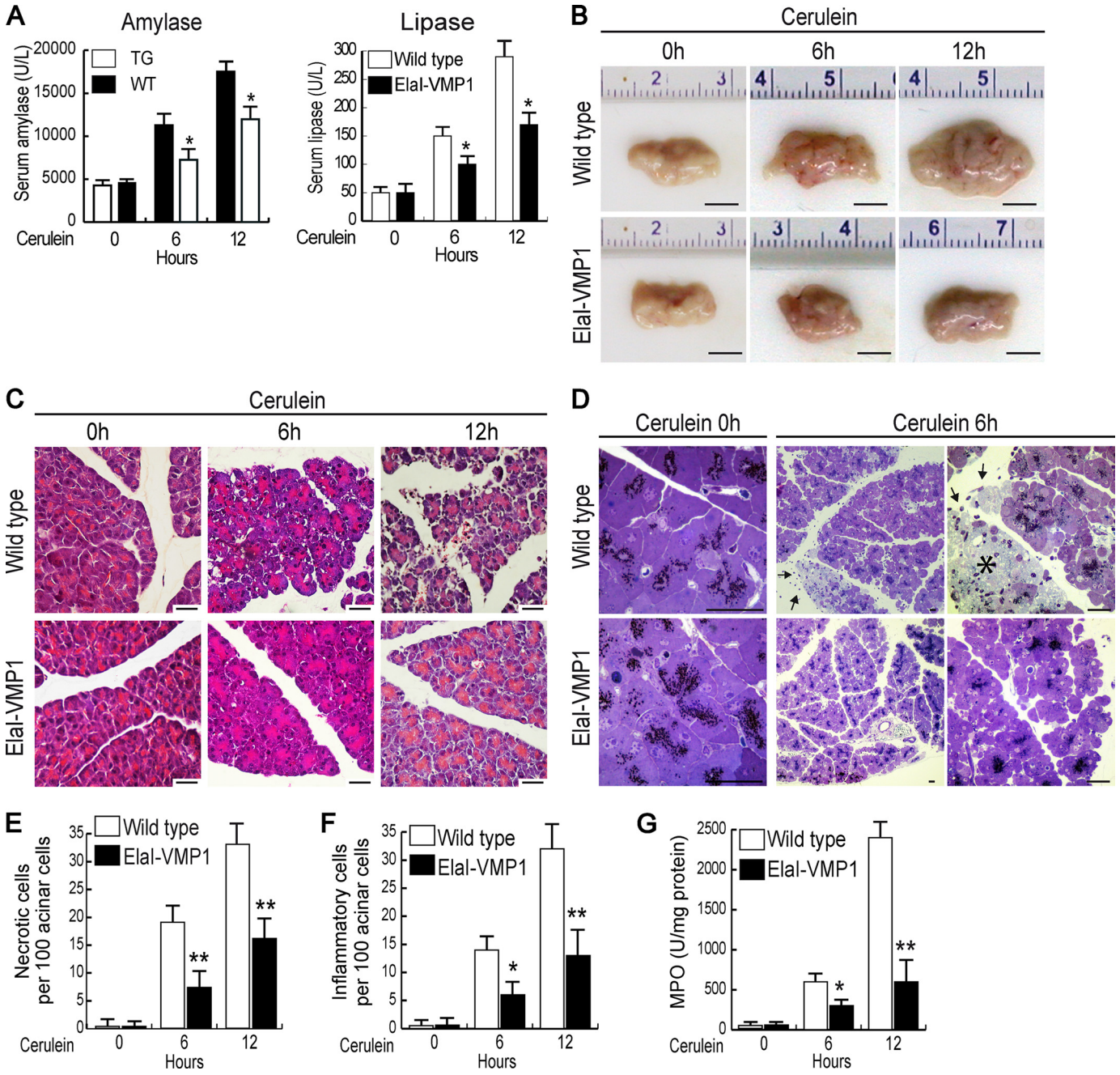

FIGURE 4. **Zymophagy protects acinar cells from trypsinogen (*TG*) activation mediated by CCK-R hyperstimulation *in vivo*.** Experimental acute pancreatitis was induced in mice by CCK-R hyperstimulation with cerulein. *A,* amylase and lipase activities in serum from wild type and ElaI-VMP1 mice after cerulein treatment in a time course scheme showing significantly reduced enzyme levels in ElaI-VMP1 mice. *B,* macroscopic photographs of freshly removed pancreata from wild type and ElaI-VMP1 mice after experimental acute pancreatitis. *C,* light microscopy of pancreatic tissue from cerulein-treated wild type and ElaI-VMP1 mice using paraffin sections stained with H&E. *D,* thin plastic section of wild type and ElaI-VMP1 pancreata stained with toluidine blue at increasing magnifications. Images show high degree of necrosis (*) as well as infiltration (*arrows*) in wild type mice after 6 h of acute pancreatitis. In contrast, almost no inflammation or evidence of necrosis is seen in cerulein-treated ElaI-VMP1 mice. *E,* necrosis quantification determined in H&E specimens as necrotic cells per 100 acinar cells. *F,* infiltration quantified in H&E specimens as number of inflammatory cells per 100 pancreatic acinar cells. *G,* myeloperoxidase (*MPO*) activity determined in pancreas homogenates. *Error bars* indicate standard deviation of at least three independent experiments (*, $p < 0.05$; **, $p < 0.001$ *versus* wild type). *Scale bars,* 0.5 cm (*B*), and 20 μm (*C* and *D*).

enzymatic levels in cerulein-treated ElaI-VMP1 mice were significantly lower compared with wild type mice. Consistently, ElaI-VMP1 mouse pancreata showed remarkably less macroscopic evidence of acute pancreatitis compared with wild type animals, which showed marked edema and hemorrhage (Fig. 4*B*). We performed light microscopy examination of cerulein-treated ElaI-VMP1 and wild type mouse pancreatic tissues through paraffin sections stained with H&E (Fig. 4*C*) and thin plastic sections stained with toluidine blue (Fig. 4*D*). Histological analyses displayed a high degree of necrosis as well as infiltration in wild type pancreata with acute pancreatitis. In contrast, neither evidence of necrosis (Fig. 4*E*) nor significant inflammation (Fig. 4, *F* and *G*) was seen in cerulein-treated ElaI-VMP1 mice. Thus, results obtained in the

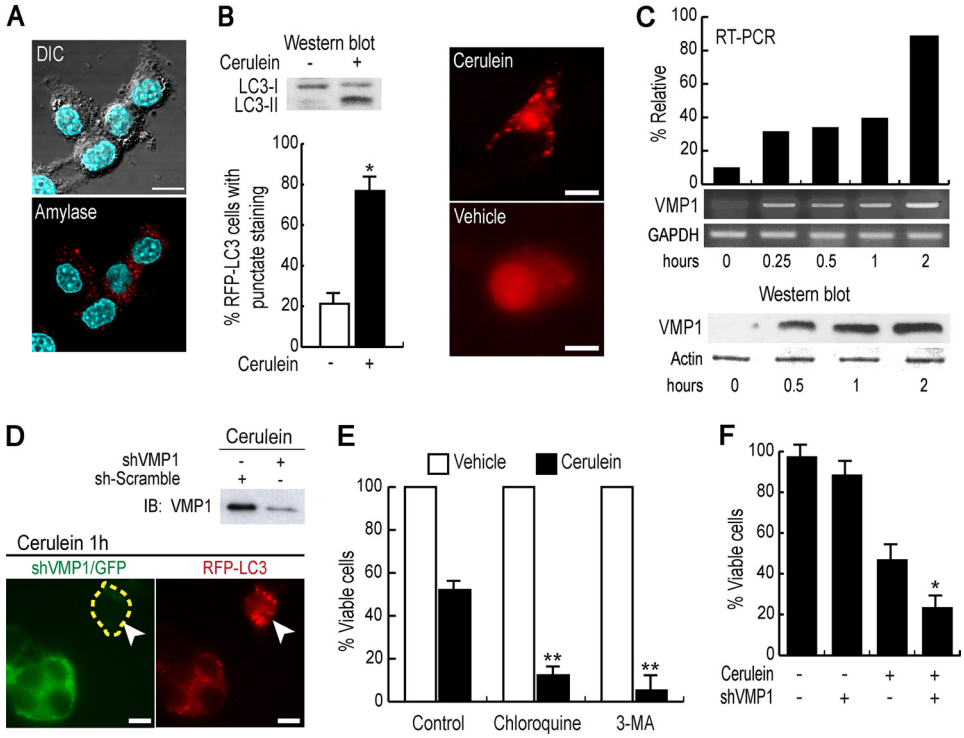

FIGURE 5. **Zymophagy prevents acinar pancreatic cell death induced by CCK-R hyperstimulation.** Rat acinar cell line AR42J differentiated by treatment with 100 nM dexamethasone. *A,* immunofluorescence assays using anti-amylase antibody evidencing presence of zymogen granules in the AR42J cell line after 48 h of dexamethasone treatment. *B,* cerulein-treated AR42J differentiated cells show LC3-I to LC3-II conversion (Western blot analysis) and RFP-LC3 aggregation, evidencing autophagy triggered by CCK-R hyperstimulation (*, $p < 0.05$ *versus* untreated). *C,* both VMP1 transcript and VMP1 protein are induced early in differentiated AR42J cells under cerulein CCK-R hyperstimulation. Results are representative of three independent experiments. *D,* shRNA mediated down-regulation of VMP1 in cerulein-treated differentiated AR42J cells cotransfected with pRFP-LC3. *Green* cells with reduced VMP1 expression show a diffuse RFP-LC3 pattern upon CCK-R hyperstimulation, indicating the absence of autophagy in VMP1 silenced cells. On the contrary, VMP1 expressing cells present aggregated RFP-LC3 in response to cerulein CCK-R hyperstimulation, evidencing autophagy induction. *E,* CCK-R hyperstimulation with cerulein promotes a nearly 50% reduction in cell viability. Disruption of the autophagy process at early steps with 3MA or at late steps with chloroquine (*CQ*) significantly decreases cell viability under CCK-R hyperstimulation (**, $p < 0.001$ *versus* control). *F,* inhibition of the VMP1-autophagy pathway by down-regulation of VMP1 expression with shVMP1 significantly decreases viability of cerulein-treated AR42J cells (*, $p < 0.05$ *versus* cerulein-treated VMP1 expressing cells). *Error bars* indicate standard deviation of at least three independent experiments. *Scale bars,* 10 μm. *DIC*, differential interference contrast.

animal model showed that zymophagy functions as a protective pathophysiological mechanism against pancreatitis-associated injury.

Zymophagy Prevents Pancreatic Acinar Cell Death Induced by CCK-R Hyperstimulation—To further understand the mechanism of zymophagy, we used the rat acinar cell line AR42J, the best characterized pancreatic acinar cell culture model. To obtain differentiated acinar cells, we treated AR42J cells with 100 nM dexamethasone (20), and granules stained positive for amylase were evidenced after 48 h of treatment (Fig. 5*A*). We used these cells to mimic the responses observed in acute pancreatitis and to recapitulate several aspects of zymophagy. In fact, CCK-R hyperstimulation induced endogenous VMP1 expression and recruited the autophagic marker RFP-LC3 (Fig. 5, *B* and *C*). We then knocked down VMP1 in this acinar cell line model using a specific short hairpin RNA construct (shVMP1) into the pCMS3-H1p-EGFP plasmid, which has a separate transcriptional cassette for EGFP to identify transfected cells (23). Knockdown experiments demonstrated that the VMP1-mediated autophagy pathway induced by CCK-R hyperstimulation is intact in this cell model, because reduced levels of this protein clearly decreased the recruitment of fluorescent RFP-LC3 (Fig. 5*D*). Subsequently, to elucidate whether zymophagy modulates cell death as a response to CCK-R hyperstimulation, we used both pharmacological and genetic (shVMP1) tools in differentiated AR42J cells. Pharmacological inhibition of autophagy initiation and autophagic flow was performed using 3-MA and chloroquine, respectively. Fig. 5*E* shows that autophagy inhibitors significantly reduced cell survival under CCK-R hyperstimulation. Moreover, VMP1 down-regulation (shVMP1) also significantly decreased acinar cell survival under CCK-R hyperstimulation (Fig. 5*F*) showing that VMP1 expression is required to prevent acinar cell death in acute pancreatitis. These results indicate that zymophagy prevents pancreatic cell death induced by the activation of zymogen granules and confirm that endogenous VMP1 expression is activated in acinar cells to mediate zymophagy as a protective cellular response against cell death.

During Zymophagy the Ubiquitin System Serves as a Targeting Signal for Zymogen Granules—Proteins involved in the recognition of target for autophagy are ubiquitin-binding proteins, such as p62, that binds directly to ubiquitin and LC3. Indeed, as shown in Fig. 2*E*, magnetically purified VMP1-mediated autophagosomes upon CCK-R hyperstimulation contain p62 and LC3 proteins. This finding suggests that the ubiquitin system may serve as a signal for the selective rec-

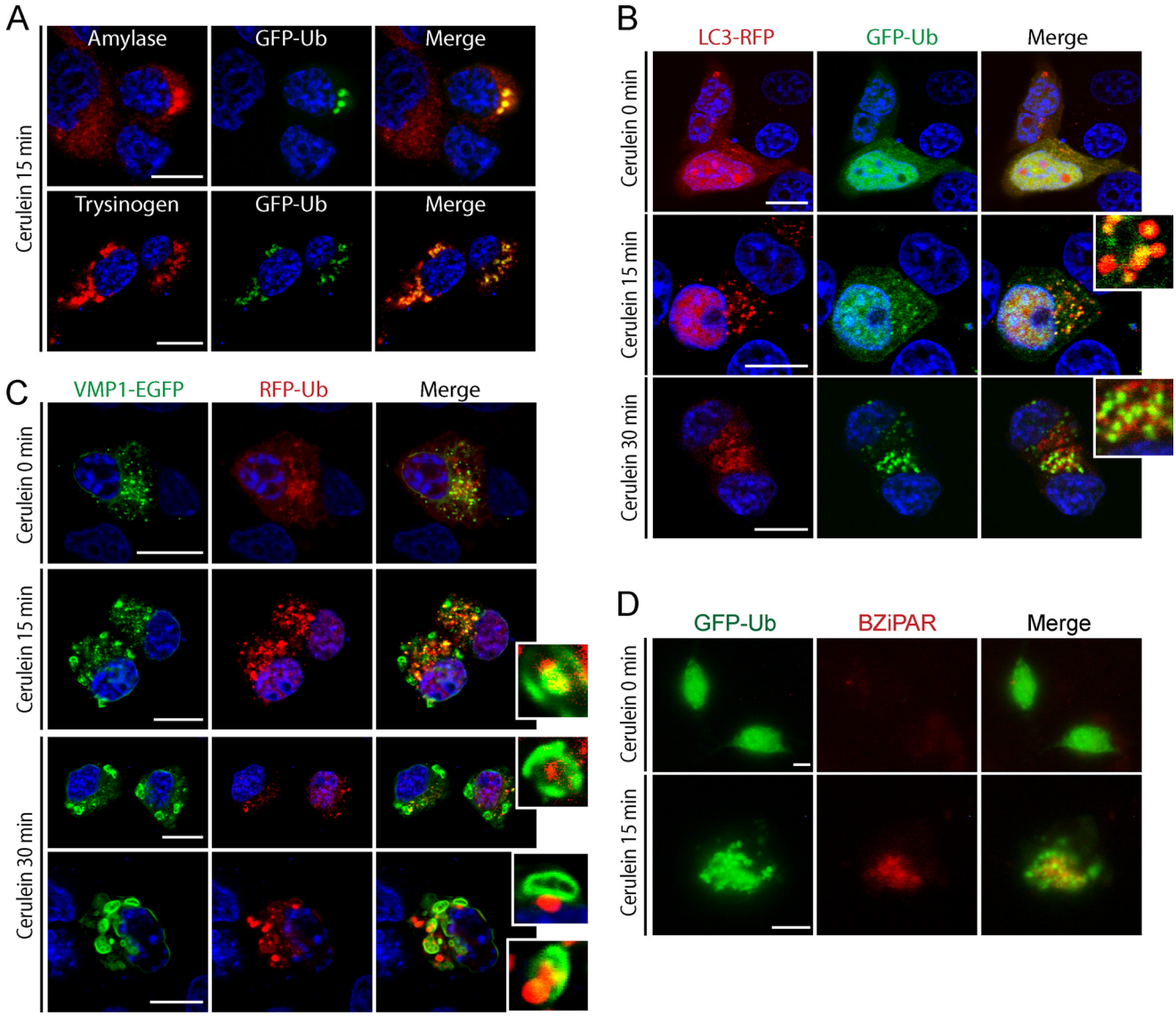

FIGURE 6. **Ubiquitin system serves as a target signal for zymogen granules during zymophagy.** Dexamethasone-differentiated AR42J cells were evaluated for ubiquitin participation in the zymophagy process. *A,* differentiated AR42J cells transfected with GFP-Ub expression plasmid were subjected to cerulein treatment for 30 min, and immunofluorescence assays were made using anti-amylase and anti-trypsinogen antibodies as zymogen granules markers. Large aggregates of ubiquitin and zymogen granules are observed in cell cytoplasm upon CCK-R hyperstimulation. *B,* acinar cells concomitantly transfected with pRFP-LC3 and GFP-Ub expression plasmids during CCK-R hyperstimulation. Both proteins remain with a diffuse pattern in untreated cells. After 15 min of cerulein treatment there is recruitment of ubiquitin inside LC3 vesicles (detailed), indicating the autophagic engulfment of ubiquitinated granules. *C,* differentiated AR42J cells cotransfected with pEGFP-VMP1 and pRFP-Ub expression plasmids. Almost no colocalization and diffuse ubiquitin pattern is shown in untreated acinar cells. Under cerulein-mediated CCK-R hyperstimulation, the engulfment of large ubiquitin aggregates by VMP1-vesicles is observed (see details on the *right*). *D,* trypsin activity evaluated by BZiPAR specific fluorescent substrate in GFP-Ub transfected acinar cells. Neither trypsin activity nor ubiquitin aggregation is evident in untreated cells. Colocalization between activated zymogen granules and ubiquitin in cerulein-treated cells indicates that ubiquitin system serves as a recognition signal during zymophagy. Results are representative of three independent experiments. *Scale bars,* 10 μm.

ognition of zymogen granules by autophagosomes during zymophagy. To test this hypothesis, we first analyzed if zymogen granules are ubiquitinated under CCK-R hyperstimulation. We transfected acinar cells with GFP-ubiquitin (GFP-Ub) expression plasmid and then performed CCK-R hyperstimulation. After 15 min of treatment, cells were fixed for immunofluorescence assays to detect ubiquitin, amylase, and trypsinogen. We found high colocalization of ubiquitin with amylase and with trypsinogen (Fig. 6*A*). We then investigated whether ubiquitinated granules are sequestered by VMP1-mediated selective autophagosomes. In complementary experiments, we concomitantly transfected acinar cells with pRFP-LC3 and GFP-Ub plasmids and then performed CCK-R hyperstimulation. Noteworthy, fluorescence analyses showed recruitment of ubiquitin and LC3 and ubiquitin signal within LC3 decorated vesicles after 15 min of treatment, indicating the autophagic engulfment of ubiquitinated granules (Fig. 6*B*). We next cotransfected cells with VMP1-EGFP and RFP-Ub to analyze if VMP1-mediated autophagosomes selectively sequester ubiquitinated granules. We found marked colocalization between VMP1 and ubiquitinated granules and engulfment of ubiquitinated granules by VMP1 vesicles. This

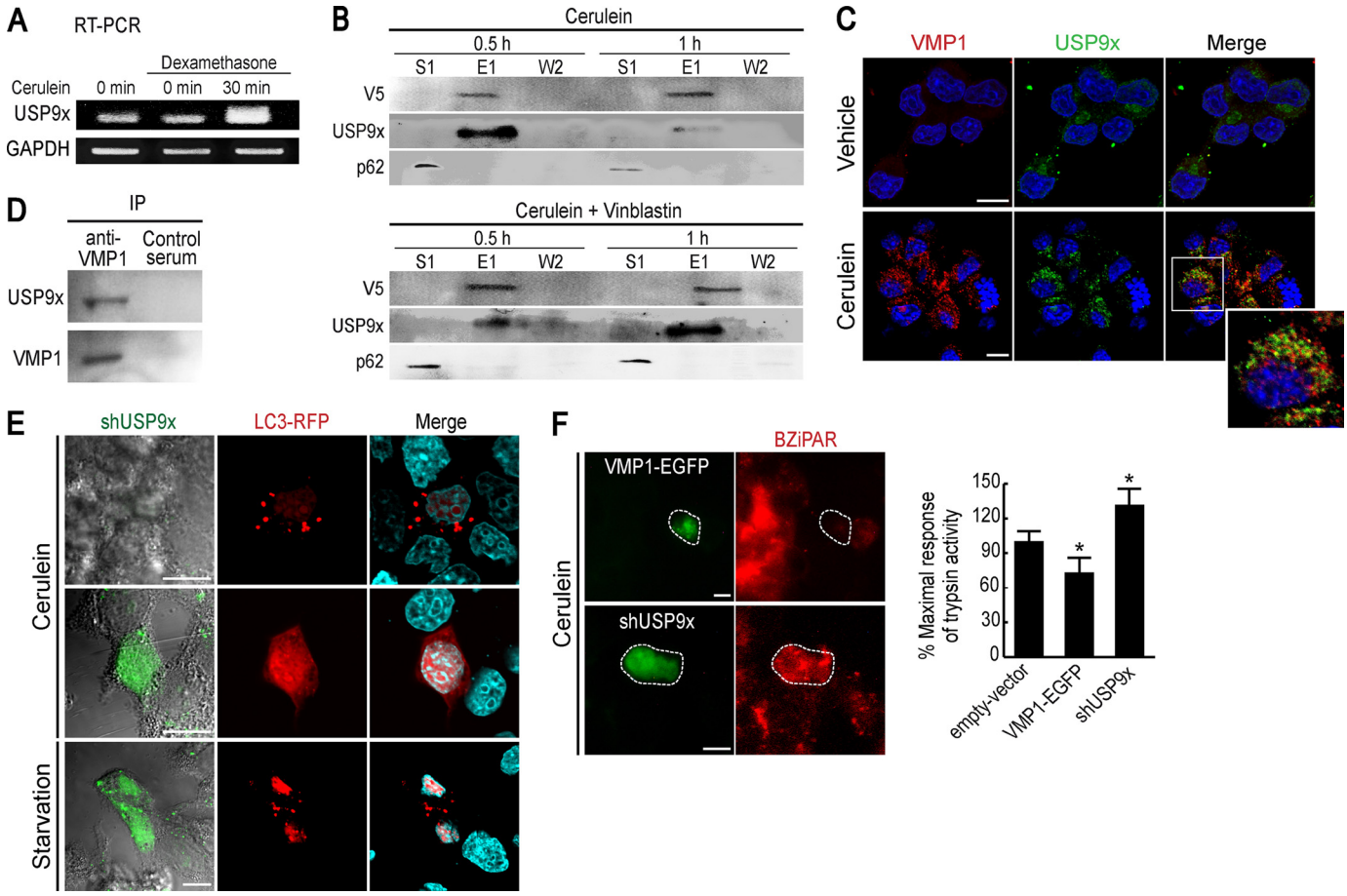

FIGURE 7. **VMP1 interacts with USP9x ubiquitin-protease, which is required for zymophagy.** *A,* RT-PCR of USP9x transcript in AR42J acinar cells. No differences in USP9x expression are observed between the nondifferentiated and dexamethasone-differentiated cells. Interestingly, USP9x expression is highly induced in dexamethasone differentiated AR42J cells under cerulein CCK-R hyperstimulation. *B,* coimmunoprecipitation assay using a VMP1-V5-His_6-tagged protein. Differentiated AR42J cells were alternatively treated with cerulein or cerulein and vinblastine. After purification, immunoblotting using anti-V5, anti-USP9x, and anti-p62 were made on the unbound fraction (*S1*), eluate (*E*), and second wash (*W2*). After 30 min of CCK-R hyperstimulation, VMP1-USP9x interaction is evident, and it decreases markedly after 1 h of cerulein treatment. Upon autophagic flow inhibition (vinblastine treatment), a higher USP9x signal is present at the 1-h cerulein treatment eluate. In none of these experiments was VMP1-p62 interaction observed. *C,* immunofluorescence assays of VMP1 and USP9x in differentiated AR42J cells shows that both proteins colocalize in vesicle structures within the zymogen granule-rich area of acinar cells after 30 min of cerulein CCK-R hyperstimulation. *D,* endogenous VMP1 and USP9x induced by CCK-R hyperstimulation coimmunoprecipitate (*IP*) in differentiated AR42J cells using anti-VMP1 antibody. *E,* cells concomitantly transfected with expression plasmids for shUSP9x and RFP-LC3, subjected to cerulein CCK-R hyperstimulation or to starvation. *Upper panel,* cells expressing USP9x show LC3 recruitment after cerulein treatment. *Middle panel,* down-regulation of USP9x (*green cell*) clearly abolished LC3 recruitment to autophagosomes after cerulein treatment. *Bottom panel,* down-regulation of USP9x (*green cell*) is not able to avoid starvation-induced LC3 recruitment. *F,* differentiated AR42J cells alternatively transfected with VMP1-EGFP or shUSP9x. Evaluation of zymogen granule activation using BZiPAR fluorescence substrate during cerulein CCK-R hyperstimulation. VMP1 expression significantly reduces the amount of trypsin activity under CCK-R hyperstimulation. The shRNA-mediated knockdown of USP9x expression significantly increases trypsin activity within acinar cells compared with untransfected cells (*, $p < 0.05$ *versus* empty vector). *Error bars* indicate standard deviation of at least three independent experiments. *Scale bars,* 10 μm.

confirms the selective sequestering of ubiquitinated zymogen granules by zymophagy (Fig. 6*C*). More importantly, we investigated if these selectively sequestered ubiquitinated granules are those activated by CCK-R hyperstimulation. We measured trypsin activity using the fluorescent substrate BZiPAR in GFP-Ub-transfected acinar cells subjected to CCK-R hyperstimulation. Fig. 6*D* shows colocalization between activated granules and ubiquitin aggregates, indicating that the ubiquitin system serves as a target signal for activated zymogen granules during zymophagy. These results demonstrate that activated granules are ubiquitinated and sequestered by the VMP1-mediated selective autophagic process and suggest that the ubiquitin system has an important role in zymophagy.

VMP1 Interacts with USP9x Ubiquitin-Protease, which Is Required for Zymophagy—Using a yeast two-hybrid screening strategy looking for VMP1 interactors, we found in 4 clones of 29 sequenced positive clones the USP9x protein (data not shown). We then studied USP9x expression in the cell model of acute pancreatitis. Interestingly, USP9x expression is highly induced in AR42J cells under CCK-R hyperstimulation (Fig. 7*A*). We also studied whether VMP1 interacts with USP9x using coimmunoprecipitation assays with a VMP1-V5-His_6-tagged protein. This experiment demonstrated that USP9x interacts with VMP1 in AR42J cells upon CCK-R hyperstimulation. The amount of coimmunoprecipitated USP9x was maximal after 0.5 h and decreased markedly after 1 h treatment (Fig. 7*B, top panel*). To further test VMP1-USP9x inter-

action, we repeated these experiments in vinblastine pretreated cells that accumulate autophagosomes. Under this condition, we observed that the USP9x-VMP1 coelution is more evident after 1 h of treatment, confirming this interaction in zymophagy (Fig. 7*B, bottom panel*). Similar experiments demonstrated that despite the fact that p62 participates in zymophagy, because it is present in magnetically purified VMP1-selective autophagosomes, this protein does not interact with VMP1 (Fig. 7*B*). We also analyzed the localization of endogenous VMP1 and USP9x in CCK-R-hyperstimulated acinar cells. Fig. 7*C* shows that endogenous VMP1 and USP9x colocalize in vesicle structures within the zymogen granule-rich area of acinar cells after 0.5 h of CCK-R hyperstimulation. We next tested whether the endogenous proteins, VMP1 and USP9x, interact during zymophagy. Using anti-VMP1 antibody, we found that endogenous VMP1 and USP9x coimmunoprecipitate in differentiated AR42J cells subjected to CCK-R hyperstimulation (Fig. 7*D*). These results further confirm the existence of a novel VMP1-USP9x interaction. To analyze the functional relevance of USP9x in zymophagy, we knocked down USP9x in the differentiated AR42J acinar cells using a specific short-hairpin RNAi construct (shUSP9x) cloned into a GFP-expressing plasmid to identify transfected cells (23). Cells were concomitantly transfected with expression plasmids for shUSP9x and RFP-LC3 and subjected to CCK-R hyperstimulation or to nutrient deprivation. Fig. 7*E* shows that USP9x down-regulation clearly abolished LC3 recruitment to autophagosomes when the selective autophagy was induced by CCK-R hyperstimulation (zymophagy). These findings indicate that USP9x is required for zymophagy. On the contrary, USP9x down-regulation failed to abolish LC3 recruitment when autophagy was induced by starvation, indicating that the identified pathway was not involved in a general form of autophagy.

Finally, we wondered if USP9x-VMP1 interaction is required for the protective role of the zymophagy process. To accomplish this objective, we evaluated zymogen granule activation during CCK-R hyperstimulation in differentiated AR42J cells using the fluorescent substrate BZiPAR. Fig. 7*F* shows that VMP1 expression significantly reduces the amount of trypsin activity under CCK-R hyperstimulation. In the same conditions, down-regulation of USP9x significantly increased trypsin activity within acinar cells. This signals that USP9x is required for the protective role of VMP1-mediated zymophagy. To summarize, our results so far suggest that zymophagy requires the ubiquitin system by implying VMP1-USP9x interaction in its protective cell function.

Structural and Biochemical Features of Zymophagy Are Preserved in Humans—Given the importance of zymophagy in acinar cells from mouse pancreata, mouse isolated pancreatic acini, and differentiated cultured cells, we investigated whether this protective and selective form of autophagy occurs in human acute pancreatitis. We studied normal and pancreatitis-affected acinar cells using immunofluorescence assays of VMP1, LC3, p62, and trypsinogen. Normal tissue areas (A_0) presented diffuse LC3 signal and undetectable VMP1 expression, evidencing very low levels of autophagy (Fig. 8*A, top row*). On the other hand, acini from pancreatitis-affected areas (A_1), in which loss of cell polarity, edema, and detachment of acinar cells are characteristic morphological features, presented marked expression of VMP1. In these areas, VMP1 highly colocalized with LC3, and VMP1-LC3 autophagosomes were observed in the granular area of acinar cells (Fig. 8*A, middle* and *bottom rows*). Quantification of LC3 recruitment and VMP1 expression confirmed that VMP1 expression is activated during human acute pancreatitis, and its expression is related to the induction of autophagosome formation in affected pancreata (Fig. 8*B*). In accordance to the already described results, VMP1-p62 colocalization further reveals the induction of the VMP1-mediated selective autophagic pathway in pancreatitis-affected human pancreatic acinar cells (Fig. 8*C*). Immunofluorescence assays for defining the localization of trypsinogen and LC3 showed the presence of autophagosomes containing zymogen granules in pancreatitis-affected acini of human specimens (Fig. 8*D*). Combined, our results demonstrate for the first time in the human pancreas the existence of VMP1-mediated selective autophagy, *i.e.* zymophagy, as a cell response to disease.

Finally, we characterized the autophagy progression in human pancreas by performing immunofluorescence assays of Lamp2, a specific lysosomal marker. In normal areas of the pancreas (A_0) small lysosomal structures are detected, whereas in affected areas (A_1) Lamp2-trypsinogen colocalization and often large lysosomal structures with no signal of trypsinogen are seen and detailed (Fig. 9). These features are characteristic of autolysosomal structures at different maturation levels, suggesting that zymophagy eventually leads to the complete degradation of sequestered zymogen granules within the autolysosome. These findings in human specimens collectively support our *in vitro* and *in vivo* results, revealing that zymophagy is an evolutionarily conserved mechanism of cellular response to disease.

DISCUSSION

Our work has led us to reveal a novel type of selective autophagy, *i.e.* zymophagy, in which VMP1 and USP9x are key functional components. Zymophagy is characterized by the formation of autophagosomes containing zymogen granules. These organelles mediate the sequestration and degradation of pancreatitis-activated zymogen granules and are induced by secretagogues and probably other stimuli in acinar cells. EM and immunofluorescence assays in human, mouse, and cultured pancreatic acinar cells show autophagic organelles at different maturation levels, suggesting that the autophagic flow progresses to acquire autolysosomal features and degrades the disease-altered secretory granules. Moreover, degradation of p62 during the course of zymophagy outlines the functionality of the autophagic pathway. These findings further confirm that selectively sequestered zymogen granules are completely degraded by zymophagy. This type of selective autophagy that is preserved in humans behaves as a protective cell mechanism against the acinar cell self-digestion and consequent progression of pancreatitis. Therefore, our investigation discloses a new selective autophagy pathway as a cellular and molecular mechanism implicated in human disease. This study also provides an insight into cell biology, demonstrating

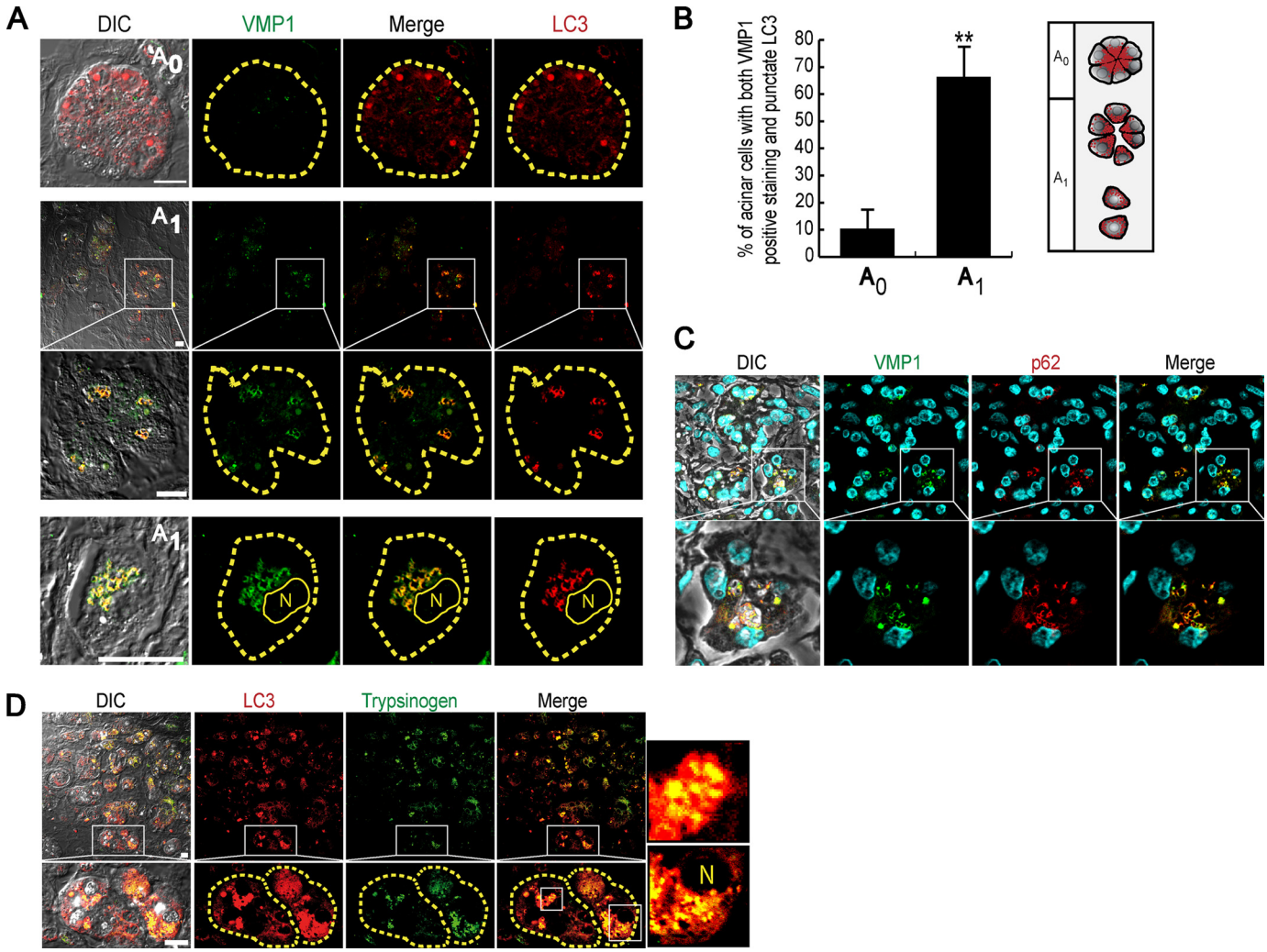

FIGURE 8. **Structural and biochemical features of zymophagy are preserved in humans.** Immunofluorescence assays of VMP1, LC3, p62, and trypsinogen in acute pancreatitis human specimens (acini are limited by *dashed lines*). *A, top row*, nonaffected acini (A_0) show diffused LC3 and undetectable VMP1. *Middle* and *bottom rows*, pancreatitis-affected areas (A_1) of human pancreas specimens show VMP1 expression that markedly colocalizes with LC3 in granular areas of acinar cells. *B,* quantification of autophagy as percentage of cells with both VMP1-positive staining and punctate LC3 per 100 acinar cells in A_0 and A_1 areas. Significant VMP1 expression colocalizing with aggregated LC3 is observed in affected tissue areas. Staining was counted in six random fields and expressed as mean ± S.D. of three independent experiments (**, $p < 0.001$ *versus* A_0). *C,* VMP1-p62 colocalization in affected tissue areas, suggests p62 participation in VMP1-mediated zymophagy in human pancreatitis (lines specify higher magnification images). *D,* LC3 and trypsinogen immunostaining in affected acini show the presence of autophagosomes containing zymogen granules (zymophagy) in pancreatitis-affected acini. When specified by *lines*, higher magnification images are shown. *Scale bars,* 10 μm. *DIC*, differential interference contrast; *N*, nucleus.

a role for the VMP1-mediated autophagy in secretory granule homeostasis and in response to cell death. This acknowledgment implicates VMP1 in a previously unknown cellular function that is distinct from its already described essential role in the early steps of autophagosome formation. Furthermore, zymophagy is a form of selective autophagy induced by hyperstimulation of G_q-coupled receptors and represents the only inducible type of autophagy described thus far in secretory cells.

The results from our work position VMP1 and p62 in the same selective autophagy pathway. Immunofluorescence assays and Western blot analyses of proteins from isolated selective autophagosomes demonstrate that these proteins colocalize and coexist in this autophagic organelle suggesting that p62 may act as a cargo receptor during the VMP1-selective autophagic pathway. The marked colocalization of ubiquitin with activated zymogen granules in the acinar cell subjected to CCK-R hyperstimulation supports this hypothesis. In addition, the localization of ubiquitin within LC3-positive, VMP1-formed autophagosomes indicates that ubiquitinated cargo is sequestered by zymophagy. Therefore, activated zymogen granules might be directly or indirectly ubiquitinated for their recognition by autophagic membranes, in which ubiquitin would act as a label for selective engulfment. This label might be subsequently removed for completing the formation of the autophagosome or even before this engulfment step. Nevertheless, our results strongly support the hypothesis that activated granules are ubiquitinated upon CCK-R hyperstimulation, and these ubiquitinated granules are sequestered by the VMP1-mediated selective autophagic pathway.

Notably, we identified USP9x as an essential component of the machinery required to selectively degraded zymogen granules during pancreatitis. The *USP9x* gene is a member of the peptidase C19 family and encodes for a ubiquitin-specific

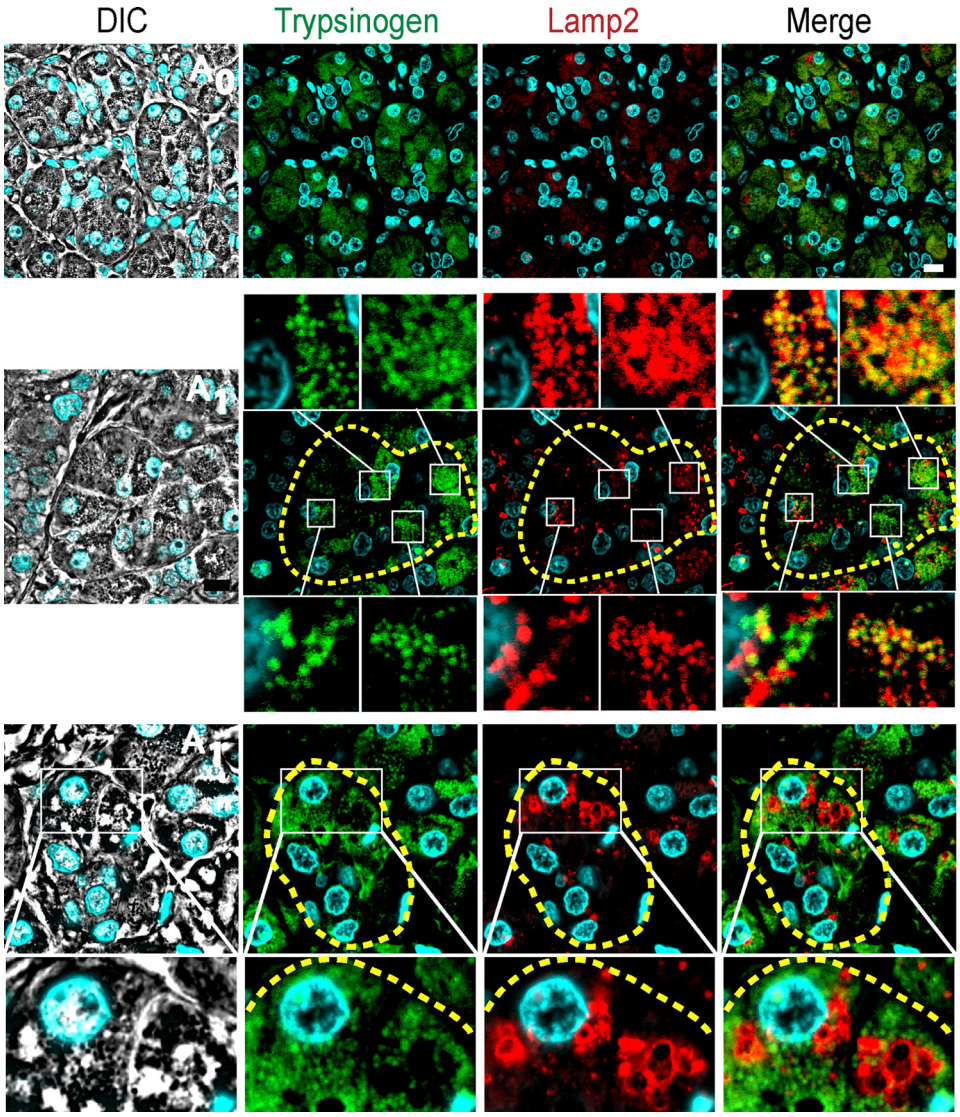

FIGURE 9. **Zymophagy leads to the complete degradation of sequestered zymogen granules within the autolysosome.** Immunofluorescence assays of Lamp2 and trypsinogen in acute pancreatitis human specimens (acini are limited by *dashed lines*). The *top row* shows small lysosomal structures labeled with Lamp2 in unaffected areas. In the *middle row*, Lamp2 and trypsinogen signals show colocalization between lysosome and zymogen granule markers. Colocalization examples are detailed, indicating that sequestered granules reach lysosomes (early autolysosomes). In the *bottom row*, Lamp2 and trypsinogen signals show large lysosomes without trypsinogen (magnification) suggesting that zymogen granules are eventually degraded in this acidic organelle (late large autolysosomes). *Lines* specify higher magnification images. Results are representative of at least three independent experiments. *Scale bars,* 10 μm.

protease. Ubiquitinating and deubiquitinating enzymes have emerged as key players in the regulation of membrane trafficking in organisms ranging from yeasts to mammals (33). Our data support the idea that there is a close cooperation between the autophagy pathway and the ubiquitin machinery required for selective autophagy. Our results demonstrate that USP9x is required to promote the selective degradation of altered zymogen granules. Interestingly, VMP1 interacts with USP9x early during zymophagy, supporting a direct functional role for this ubiquitin-specific protease in this selective autophagic pathway. Furthermore, down-regulation of USP9x abolished activated zymogen granule degradation in acinar cells under CCK-R hyperstimulation, confirming the essential role of VMP1-USP9x interaction for zymophagy. USP9x is likely to modulate zymogen granule-selective engulfment during acute pancreatitis by modulating VMP1 or providing a preferential recognition signal for altered zymogen granules. These data demonstrate for the first time that ubiquitin modifications may possess an additional function in acinar cells by promoting the degradation of highly harmful activated zymogen granules. Alternatively, both ubiquitination and deubiquitination of distinct critical molecules might be required for selective autophagy. Thus, because of the potential importance of this type of regulation, this study may fuel future investigations aimed to identify the potential E3 ligases and ubiquitinated substrate(s) required for zymophagy.

Our findings provide further understanding of the molecular mechanisms relevant to human diseases, particularly acute pancreatitis. This condition has classically been considered an autodigestive disorder where the inappropriate activation of trypsinogen within the pancreatic acinar cell leads to the pro-

gression of the disease. However, the exact mechanism for the initiation of zymogen granule activation remains a subject of intensive investigation and debate after more than 5 decades of research efforts (34, 35). Similarly, the role of autophagy in pancreatitis is seemingly incomplete, sometimes contradictory, and requires further investigations. For instance, Hashimoto *et al.* (36) and Mareninova *et al.* (37) propose that autophagy is responsible for the zymogen activation within the acinar cell during acute pancreatitis. These suggestions are based on the finding that deletion of the *Atg5* gene in pancreatic cells prevents acute pancreatitis. Unfortunately, this observation is currently questioned by the knowledge that ATG5 has other implications not related to autophagy; in fact, when proteolytically activated, it becomes a pro-apoptotic molecule (38). Moreover, cells lacking *Atg5* and *Atg7* can still perform autophagy-mediated protein degradation (39), demonstrating that deletion of these genes does not completely abolish autophagy. These data also introduce the question whether the role of different types of autophagy, similar to the one remaining in the *Atg5* knock-out mice, have an impact on pancreatitis. In this regard, we describe that this selective form of VMP1-induced autophagy (zymophagy), triggered by CCK-R hyperstimulation, is not inhibited, sequesters activated zymogen granules, and protects from acute pancreatitis. Therefore, these results significantly extend our current knowledge on autophagy by demonstrating that the outcome of pancreatitis differs when different types of autophagy pathways are considered, including selective and nonselective ones.

Our results demonstrate also for the first time that there is activation of the VMP1-autophagic pathway and zymophagy during human pancreatitis. These findings lead us to discuss how this knowledge fits the current theoretical framework regarding the occurrence and progression of this disease. Acute pancreatitis is a frequent, painful, and often deadly disease that ranges from a mild, edematous, and autolimited process to a severe necrotizing and eventually lethal condition. Additionally, the etiology of this disease is diverse, and different stimuli can initiate the same autodigestion cascade via different mechanisms (40). Our data show that there is expression of VMP1 during acute pancreatitis in humans, and there is formation of autophagosomes where p62, LC3, and zymogen granules colocalize. Altogether, our findings indicate that zymophagy also occurs in human pancreatitis. This protective cell response could explain, at least in part, the auto-limited form of this disease seen in many patients. Hence, it is tempting to speculate that the more efficient zymophagic response by the pancreatic acinar cell, the less severity of the disease. In contrast, severe forms of pancreatitis offering an excess of cargo and an accelerated rate of degradation might overcome or disrupt the protective capacity of this selective autophagic process. The latter possibility is suggested by our results because the inhibition of the autophagic flow impairs the protective role of zymophagy. The findings of Fortunato and Kroemer (41), regarding the reduction of the autophagosome-lysosome fusion in human alcoholic pancreatitis, further support our hypothesis.

Finally, this novel autophagic pathway that selectively degrades altered secretory granules might be involved in other pathological processes affecting secretory cells, such as pancreatic beta cells in diabetes mellitus or Paneth cells in Crohn disease. Therefore, more studies on autophagy as a programmed cell response to pathological processes that affect protein secretion are important to significantly expand our knowledge of the role of autophagy in both cell biology and human disease.

Acknowledgments—We are grateful to Dr. Celina Morales (Dept. of Pathology, School of Medicine, University of Buenos Aires) for expert help in human pancreas histopathological analysis. We thank Dr. Natalia Causada Calo for assistance in the drafting of the manuscript.

REFERENCES

1. Kraft, C., Peter, M., and Hofmann, K. (2010) *Nat. Cell Biol.* **12,** 836–841
2. Suzuki, K., and Ohsumi, Y. (2007) *FEBS Lett.* **581,** 2156–2161
3. Kraft, C., Reggiori, F., and Peter, M. (2009) *Biochim. Biophys. Acta* **1793,** 1404–1412
4. Pankiv, S., Clausen, T. H., Lamark, T., Brech, A., Bruun, J. A., Outzen, H., Øvervatn, A., Bjørkøy, G., and Johansen, T. (2007) *J. Biol. Chem.* **282,** 24131–24145
5. Kim, P. K., Hailey, D. W., Mullen, R. T., and Lippincott-Schwartz, J. (2008) *Proc. Natl. Acad. Sci. U.S.A.* **105,** 20567–20574
6. Kraft, C., Deplazes, A., Sohrmann, M., and Peter, M. (2008) *Nat. Cell Biol.* **10,** 602–610
7. Ropolo, A., Grasso, D., Pardo, R., Sacchetti, M. L., Archange, C., Lo Re, A., Seux, M., Nowak, J., Gonzalez, C. D., Iovanna, J. L., and Vaccaro, M. I. (2007) *J. Biol. Chem.* **282,** 37124–37133
8. Tian, Y., Li, Z., Hu, W., Ren, H., Tian, E., Zhao, Y., Lu, Q., Huang, X., Yang, P., Li, X., Wang, X., Kovács, A. L., Yu, L., and Zhang, H. (2010) *Cell* **141,** 1042–1055
9. Itakura, E., and Mizushima, N. (2010) *Autophagy* **6,** 764–776
10. Calvo-Garrido, J., and Escalante, R. (2010) *Autophagy* **6,** 100–109
11. Hofbauer, B., Saluja, A. K., Lerch, M. M., Bhagat, L., Bhatia, M., Lee, H. S., Frossard, J. L., Adler, G., and Steer, M. L. (1998) *Am. J. Physiol.* **275,** G352–G362
12. Williams, J. A. (2008) *Curr. Opin. Gastroenterol.* **24,** 573–579
13. Fernandez-Zapico, M. E., Mladek, A., Ellenrieder, V., Folch-Puy, E., Miller, L., and Urrutia, R. (2003) *EMBO J.* **22,** 4748–4758
14. Cox, B., and Emili, A. (2006) *Nat. Protoc.* **1,** 1872–1878
15. Howell, K. E., Schmid, R., Ugelstad, J., and Gruenberg, J. (1989) *Methods Cell Biol.* **31,** 265–292
16. Saluja, A. K., Bhagat, L., Lee, H. S., Bhatia, M., Frossard, J. L., and Steer, M. L. (1999) *Am. J. Physiol.* **276,** G835–G842
17. Chanson, M., Bruzzone, R., Bosco, D., and Meda, P. (1989) *J. Cell. Physiol.* **139,** 147–156
18. DiMagno, M. J., Williams, J. A., Hao, Y., Ernst, S. A., and Owyang, C. (2004) *Am. J. Physiol. Gastrointest. Liver Physiol.* **287,** G80–G87
19. Dawra, R., Ku, Y. S., Sharif, R., Dhaulakhandi, D., Phillips, P., Dudeja, V., and Saluja, A. K. (2008) *Pancreas* **37,** 62–68
20. Suzuki, K., Ota, H., Sasagawa, S., Sakatani, T., and Fujikura, T. (1983) *Anal. Biochem.* **132,** 345–352
21. De Lisle, R. C., Norkina, O., Roach, E., and Ziemer, D. (2005) *Am. J. Physiol. Cell Physiol.* **289,** C1169–C1178
22. Dantuma, N. P., Groothuis, T. A., Salomons, F. A., and Neefjes, J. (2006) *J. Cell Biol.* **173,** 19–26
23. Bergink, S., Salomons, F. A., Hoogstraten, D., Groothuis, T. A., de Waard, H., Wu, J., Yuan, L., Citterio, E., Houtsmuller, A. B., Neefjes, J., Hoeijmakers, J. H., Vermeulen, W., and Dantuma, N. P. (2006) *Genes Dev.* **20,** 1343–1352
24. Gomez, T. S., Hamann, M. J., McCarney, S., Savoy, D. N., Lubking,

C. M., Heldebrant, M. P., Labno, C. M., McKean, D. J., McNiven, M. A., Burkhardt, J. K., and Billadeau, D. D. (2005) *Nat. Immunol.* **6,** 261–270
25. Seibenhener, M. L., Geetha, T., and Wooten, M. W. (2007) *FEBS Lett.* **581,** 175–179
26. Moscat, J., Diaz-Meco, M. T., and Wooten, M. W. (2007) *Trends Biochem. Sci.* **32,** 95–100
27. Criddle, D. N., Gerasimenko, J. V., Baumgartner, H. K., Jaffar, M., Voronina, S., Sutton, R., Petersen, O. H., and Gerasimenko, O. V. (2007) *Cell Death Differ.* **14,** 1285–1294
28. Halangk, W., Krüger, B., Ruthenbürger, M., Stürzebecher, J., Albrecht, E., Lippert, H., and Lerch, M. M. (2002) *Am. J. Physiol. Gastrointest. Liver Physiol.* **282,** G367–G374
29. Krüger, B., Albrecht, E., and Lerch, M. M. (2000) *Am. J. Pathol.* **157,** 43–50
30. Raraty, M., Ward, J., Erdemli, G., Vaillant, C., Neoptolemos, J. P., Sutton, R., and Petersen, O. H. (2000) *Proc. Natl. Acad. Sci. U.S.A.* **97,** 13126–13131
31. Thrower, E., Husain, S., and Gorelick, F. (2008) *Curr. Opin. Gastroenterol.* **24,** 580–585
32. Niederau, C., Ferrell, L. D., and Grendell, J. H. (1985) *Gastroenterology* **88,** 1192–1204
33. Millard, S. M., and Wood, S. A. (2006) *J. Cell Biol.* **173,** 463–468
34. Gaisano, H. Y., and Gorelick, F. S. (2009) *Gastroenterology* **136,** 2040–2044
35. Vaccaro, M. I. (2008) *Pancreatology* **8,** 425–429
36. Hashimoto, D., Ohmuraya, M., Hirota, M., Yamamoto, A., Suyama, K., Ida, S., Okumura, Y., Takahashi, E., Kido, H., Araki, K., Baba, H., Mizushima, N., and Yamamura, K. (2008) *J. Cell Biol.* **181,** 1065–1072
37. Mareninova, O. A., Hermann, K., French, S. W., O'Konski, M. S., Pandol, S. J., Webster, P., Erickson, A. H., Katunuma, N., Gorelick, F. S., Gukovsky, I., and Gukovskaya, A. S. (2009) *J. Clin. Invest.* **119,** 3340–3355
38. Pyo, J. O., Jang, M. H., Kwon, Y. K., Lee, H. J., Jun, J. I., Woo, H. N., Cho, D. H., Choi, B., Lee, H., Kim, J. H., Mizushima, N., Oshumi, Y., and Jung, Y. K. (2005) *J. Biol. Chem.* **280,** 20722–20729
39. Nishida, Y., Arakawa, S., Fujitani, K., Yamaguchi, H., Mizuta, T., Kanaseki, T., Komatsu, M., Otsu, K., Tsujimoto, Y., and Shimizu, S. (2009) *Nature* **461,** 654–658
40. Sherwood, M. W., Prior, I. A., Voronina, S. G., Barrow, S. L., Woodsmith, J. D., Gerasimenko, O. V., Petersen, O. H., and Tepikin, A. V. (2007) *Proc. Natl. Acad. Sci. U.S.A.* **104,** 5674–5679
41. Fortunato, F., and Kroemer, G. (2009) *Autophagy* **5,** 850–853